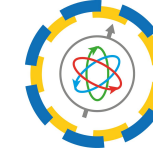




JAGIELLONIAN UNIVERSITY
IN KRAKÓW

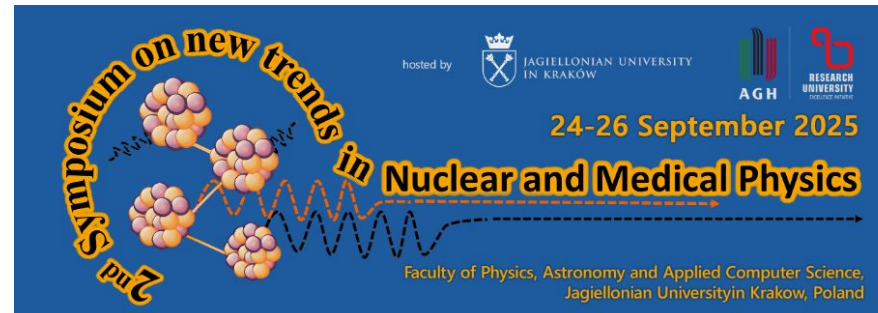


J-PET

Range Monitoring in Proton Therapy

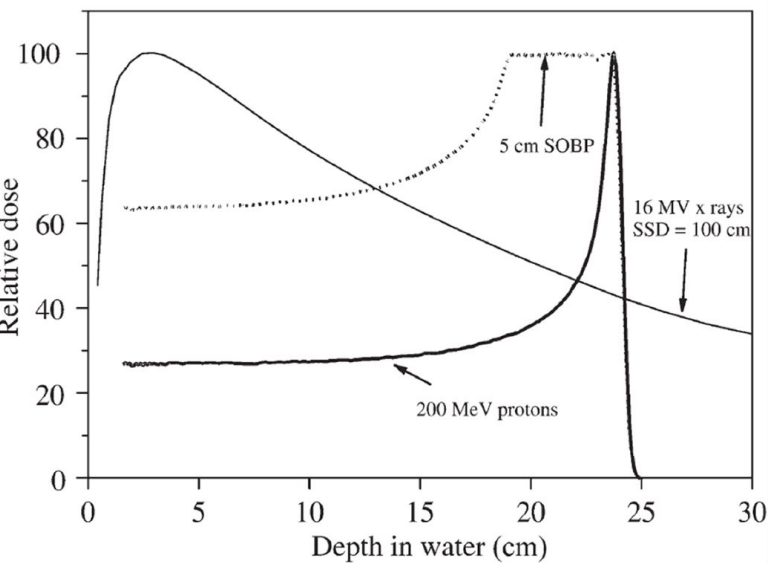
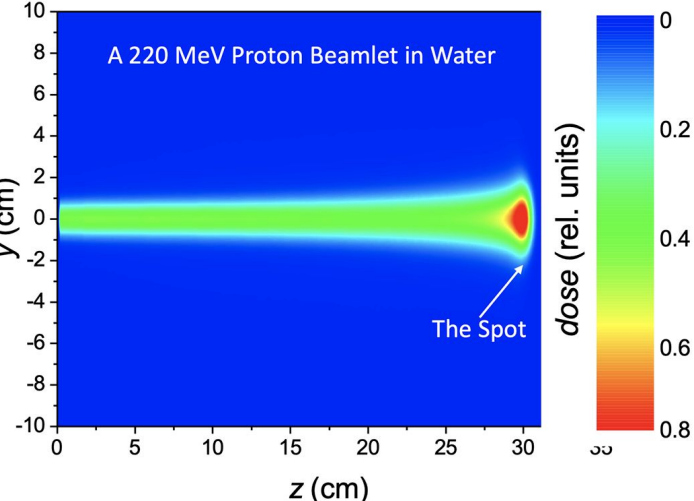
Using the J-PET Scanner: First Experimental Insights

Szymon Niedźwiecki
on behalf of the J-PET collaboration



Proton therapy

- Protons deposit most energy at the Bragg peak leading to a sharp distal dose fall-off.
- Enables high tumor dose with reduced integral dose to adjacent normal tissues.
- Dosimetric advantage forms the rationale for proton therapy.



Proton range determination

Main sources of uncertainty:

- morphological changes,
- anatomical deformation due to motion
- HU to RSP conversion error

Proton range determination

Main sources of uncertainty:

- morphological changes,
- anatomical deformation due to motion
- HU to RSP conversion error

1. Dual-energy CT (DECT) / photon-counting

CT (PCCT)

Charles Ekene Chika, World J Radiol. 2025 Jun 28;17(6):105728. doi: 10.4329/wjr.v17.i6.105728

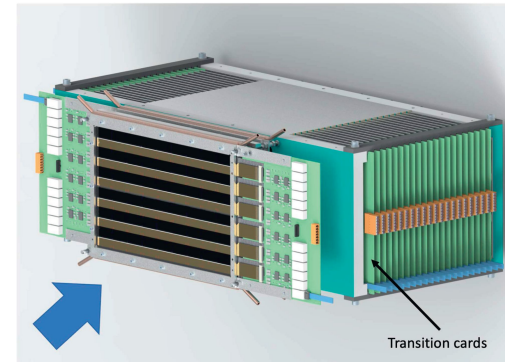
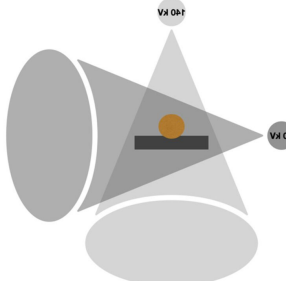
2. Proton CT (pCT) / proton radiography (pRad)

Alme J, et al.(2020) A High-Granularity Digital Tracking Calorimeter Optimized for Proton CT.

Front. Phys. 8:568243. doi: 10.3389/fphy.2020.568243

3. Machine learning & Monte-Carlo aid

Wildman VL, et al. Recent advances in applying machine learning to proton radiotherapy. Biomed Phys Eng Express. 2025 Jul 23;11(4):042005. doi: 10.1088/2057-1976/adeb90. PMID: 40609552; PMCID: PMC12284894.



Proton range determination

1. Dual-energy CT (DECT) / photon-counting

CT (PCCT)

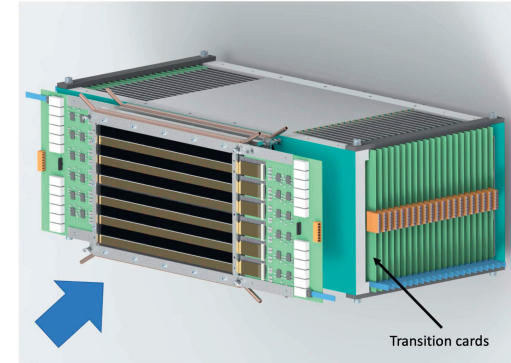
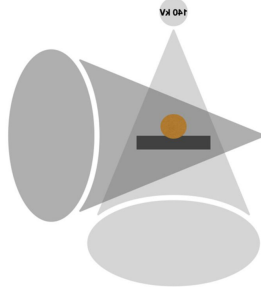
Charles Ekene Chika, World J Radiol. 2025 Jun 28;17(6):105728. doi: 10.4329/wjr.v17.i6.105728

2. Proton CT (pCT) / proton radiography (pRad)

Alme J, et al.(2020) A High-Granularity Digital Tracking Calorimeter Optimized for Proton CT. Front. Phys. 8:568243. doi: 10.3389/fphy.2020.568243

3. Machine learning & Monte-Carlo aid

Wildman VL, et al.. Recent advances in applying machine learning to proton radiotherapy. Biomed Phys Eng Express. 2025 Jul 23;11(4):042005. doi: 10.1088/2057-1976/adeb90. PMID: 40609552; PMCID: PMC12284894.



Main sources of uncertainty:

- morphological changes,
- anatomical deformation due to motion
- HU to RSP conversion error

1. Prompt Gamma Imaging (PGI) / Prompt Gamma Spectroscopy (PGS) / Prompt Gamma Timing (PGT)

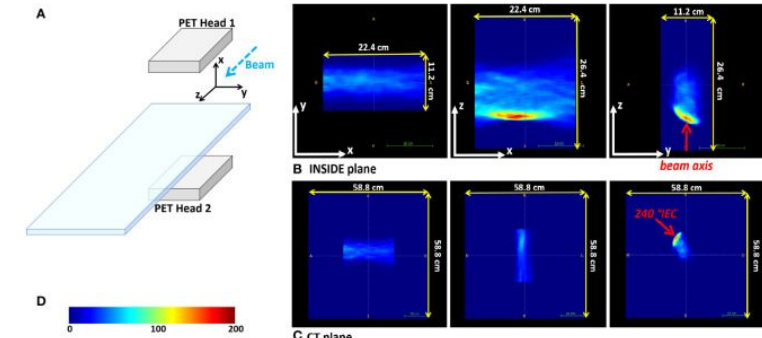
Everaere P, et al. Prompt gamma energy integration: a new method for online-range verification in proton therapy with pulsed-beams. Front. Phys. 12:1371015. doi: 10.3389/fphy.2024.1371015

2. Ionoacoustic / protoacoustic imaging

Alme J, et Wang S, et al. Real-time tracking of the Bragg peak during proton therapy via 3D protoacoustic Imaging in a clinical scenario. Npj Imaging. 2024;2(1):34. doi: 10.1038/s44303-024-00039-x. Epub 2024 Sep 17. PMID: 40078731; PMCID: PMC11893450.

3. In-beam PET and delayed gamma imaging

Moglionico M, et al. In-vivo range verification analysis with in-beam PET data for patients treated with proton therapy at CNAO. Front Oncol. 2022 Sep 26;12:929949. doi: 10.3389/fonc.2022.929949. PMID: 36226070; PMCID: PMC9549776.



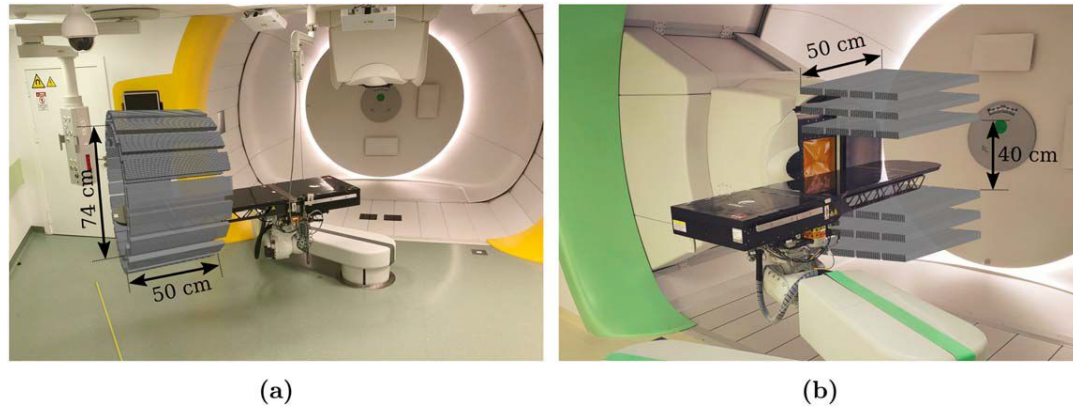
Physics in Medicine & Biology



PAPER

Detection of range shifts in proton beam therapy using the J-PET scanner: a patient simulation study

Karol Brzeziński^{1,2,*}, Jakub Baran^{3,4,5}, Damian Borys^{6,7}, Jan Gajewski¹, Neha Chug^{3,4,5}, Aurélien Coussat^{3,4,5}, Eryk Czerwiński^{3,4,5}, Meysam Dadgar^{3,4,5}, Kamil Dulski^{3,4,5}, Kavya V. Eliyan^{3,4,5}, Aleksander Gajos^{3,4,5}, Krzysztof Kapczak^{3,4,5}, Łukasz Kaplon^{3,4,5}, Konrad Klimaszewski³, Paweł Konieczka³, Renata Kopeć³, Grzegorz Korczył^{3,4,5}, Tomasz Kozik^{3,4,5}, Wojciech Krzemień⁹, Deepak Kumar^{4,5}, Antony J. Lomax^{10,11}, Keegan McNamara^{10,11}, Szymon Niedźwiecki^{3,4,5}, Paweł Olko³, Dominik Panek^{3,4,5}, Szymon Parzych^{3,4,5}, Elena Perez del Rio^{3,4,5}, Lech Raczyński³, Sushil Sharma^{3,4,5}, Shivani^{3,4,5}, Roman Y. Shopa³, Tomasz Skóra¹², Małgorzata Skurzok^{3,4,5}, Paulina Stasica¹⁰, Ewa Ł. Stępień^{3,4,5}, Keyvan Tayefi^{3,4,5}, Faranak Tayefi^{3,4,5}, Damien C. Weber^{10,13,14}, Carla Winterhalter^{10,11}, Wojciech Wiślicki⁸, Paweł Moskal^{3,4,5} and Antoni Ruciński³



(a)

(b)

Physica Medica 118 (2024) 103301

Contents lists available at ScienceDirect

Physica Medica

journal homepage: www.elsevier.com/locate/ejmp

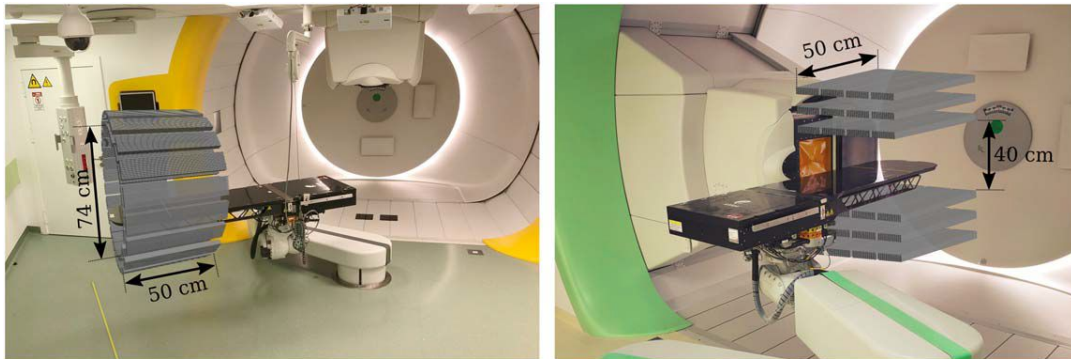
Technical note

Feasibility of the J-PET to monitor the range of therapeutic proton beams

Jakub Baran^{3,4,5,7}, Damian Borys^{3,4,5,7}, Karol Brzeziński^{1,6}, Jan Gajewski¹, Michał Siliarski^{3,4,5,7}, Neha Chug^{3,4,5,7}, Aurélien Coussat^{3,4,5,7}, Eryk Czerwiński^{3,4,5,7}, Meysam Dadgar^{3,4,5,7}, Kamil Dulski^{3,4,5,7}, Kavya V. Eliyan^{3,4,5,7}, Aleksander Gajos^{3,4,5,7}, Krzysztof Kapczak^{3,4,5,7}, Łukasz Kaplon^{3,4,5,7}, Konrad Klimaszewski³, Paweł Konieczka³, Renata Kopeć³, Grzegorz Korczył^{3,4,5,7}, Tomasz Kozik^{3,4,5,7}, Wojciech Krzemień¹, Deepak Kumar^{3,4,5,7}, Antony J. Lomax^{1,6}, Keegan McNamara^{1,6}, Szymon Niedźwiecki^{3,4,5,7}, Paweł Olko³, Dominik Panek^{3,4,5,7}, Szymon Parzych^{3,4,5,7}, Elena Perez del Rio^{3,4,5,7}, Lech Raczyński³, Sushil Sharma^{3,4,5,7}, Shivani^{3,4,5,7}, Roman Y. Shopa³, Tomasz Skóra^{1,6}, Małgorzata Skurzok^{3,4,5,7}, Paulina Stasica^{1,6}, Ewa Ł. Stępień^{3,4,5,7}, Keyvan Tayefi^{3,4,5,7}, Faranak Tayefi^{3,4,5,7}, Damien C. Weber^{1,6,14}, Carla Winterhalter^{1,6}, Wojciech Wiślicki⁸, Paweł Moskal^{3,4,5,7}, Antoni Ruciński³

PAPER
Detection of range shifts in proton beam therapy using the J-PET scanner: a patient simulation study

Karol Brzeziński^{1,2,*}, Jakub Baran^{3,4,5}, Damian Borys^{6,7}, Jan Gajewski¹, Neha Chug^{3,4,5}, Aurelien Coussat^{3,4,5}, Eryk Czerwiński^{3,4,5}, Meysam Dadgar^{3,4,5}, Kamil Dulski^{3,4,5}, Kavya V. Eliyan^{3,4,5}, Aleksander Gajos^{3,4,5}, Krzysztof Kapczak^{3,4,5}, Łukasz Kaplon^{3,4,5}, Konrad Klimaszewski³, Paweł Konieczka³, Renata Kopeć³, Grzegorz Korcyl^{3,4,5}, Tomasz Kozik^{3,4,5}, Wojciech Krzemień⁹, Deepak Kumar^{3,4,5}, Antony J. Lomax^{10,11}, Keegan McNamara^{10,11}, Szymon Niedźwiecki^{3,4,5}, Paweł Olko³, Dominik Panek^{3,4,5}, Szymon Parzych^{3,4,5}, Elena Perez del Rio^{3,4,5}, Lech Raczyński³, Sushil Sharma^{3,4,5}, Shivani^{3,4,5}, Roman Y. Shopa³, Tomasz Skóra¹², Małgorzata Skurzok^{3,4,5}, Paulina Stasica¹⁰, Ewa Ł. Stępień^{3,4,5}, Keyvan Tayefi^{3,4,5}, Faranak Tayefi^{3,4,5}, Damien C. Weber^{10,13,14}, Carla Winterhalter^{10,11}, Wojciech Wiślicki⁸, Paweł Moskal^{3,4,5} and Antoni Ruciński³

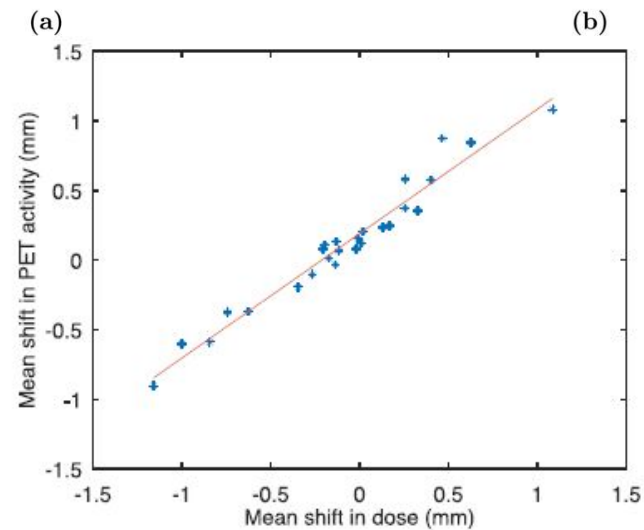

Physica Medica 118 (2024) 103301

Contents lists available at ScienceDirect

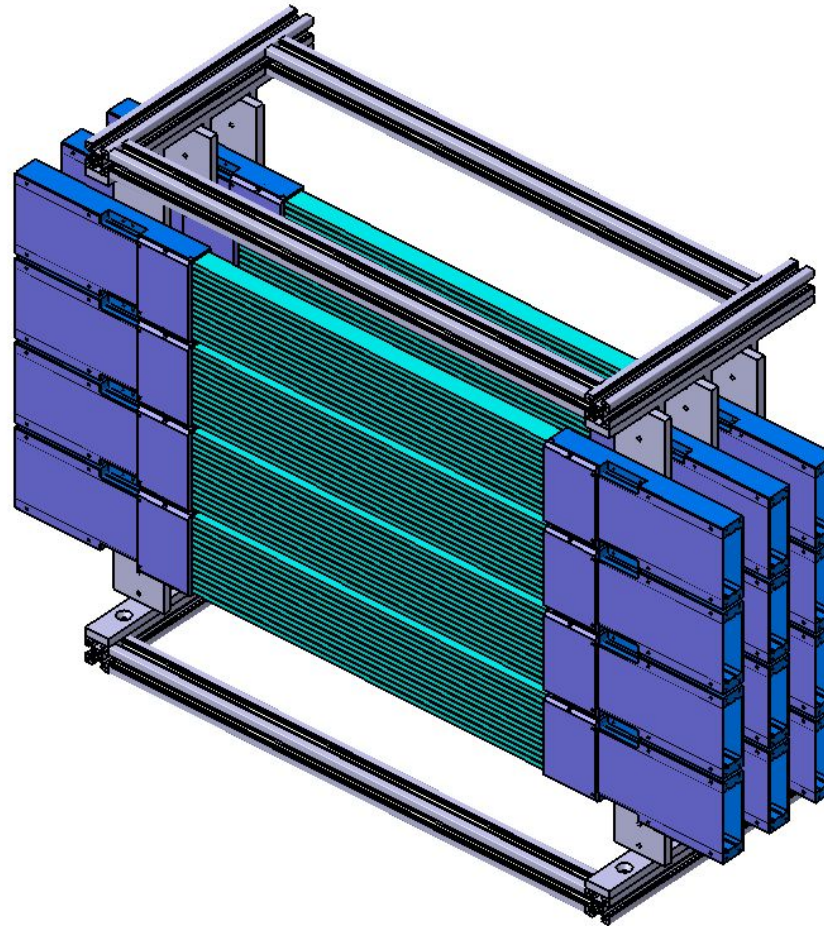
Physica Medica

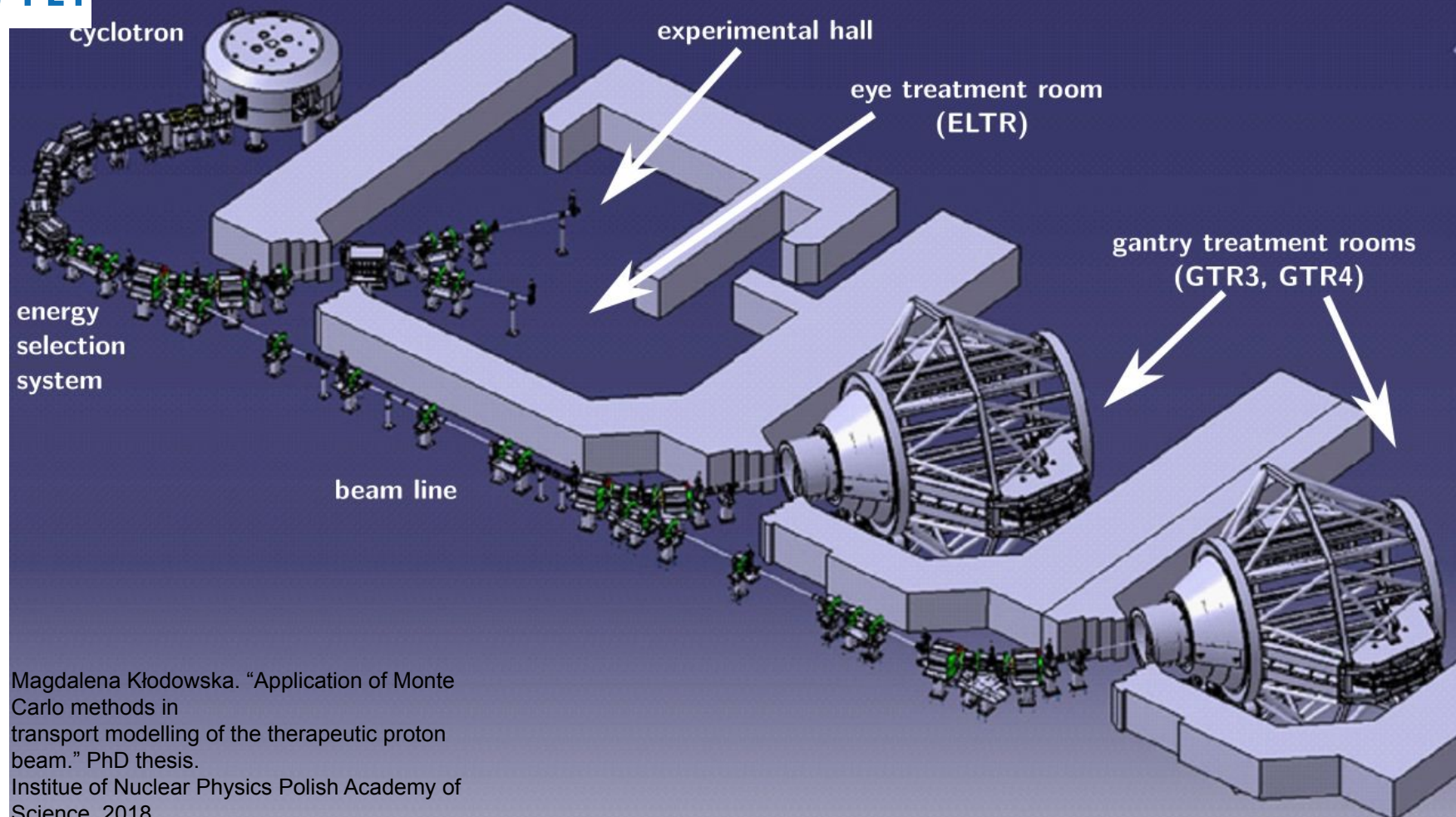
 journal homepage: www.elsevier.com/locate/ejmp
Technical note
Feasibility of the J-PET to monitor the range of therapeutic proton beams

Jakub Baran^{3,4,5,6}, Damian Borys^{3,4,5}, Karol Brzeziński^{1,6}, Jan Gajewski¹, Michał Siliński^{3,4,5,6}, Neha Chug^{3,4,5,6}, Aurelien Coussat^{3,4,5,6}, Eryk Czerwiński^{3,4,5,6}, Meysam Dadgar^{3,4,5,6}, Kamil Dulski^{3,4,5,6}, Kavya V. Eliyan^{3,4,5,6}, Aleksander Gajos^{3,4,5,6}, Krzysztof Kapczak^{3,4,5,6}, Łukasz Kaplon^{3,4,5,6}, Konrad Klimaszewski³, Paweł Konieczka³, Renata Kopeć³, Grzegorz Korcyl^{3,4,5,6}, Tomasz Kozik^{3,4,5,6}, Wojciech Krzemień¹, Deepak Kumar^{3,4,5,6}, Antony J. Lomax^{1,6}, Keegan McNamara^{1,6}, Szymon Niedźwiecki^{3,4,5,6}, Paweł Olko³, Dominik Panek^{3,4,5,6}, Szymon Parzych^{3,4,5,6}, Elena Perez del Rio^{3,4,5,6}, Lech Raczyński³, Moyo Simbarashe^{3,4,5,6}, Sushil Sharma^{3,4,5,6}, Shivani^{3,4,5,6}, Roman Y. Shopa³, Tomasz Skóra^{1,6}, Małgorzata Skurzok^{3,4,5,6}, Paulina Stasica^{1,6}, Ewa Ł. Stępień^{3,4,5,6}, Keyvan Tayefi^{3,4,5,6}, Faranak Tayefi^{3,4,5,6}, Damien C. Weber^{1,6}, Carla Winterhalter^{1,6}, Wojciech Wiślicki⁸, Paweł Moskal^{3,4,5,6}, Antoni Ruciński³

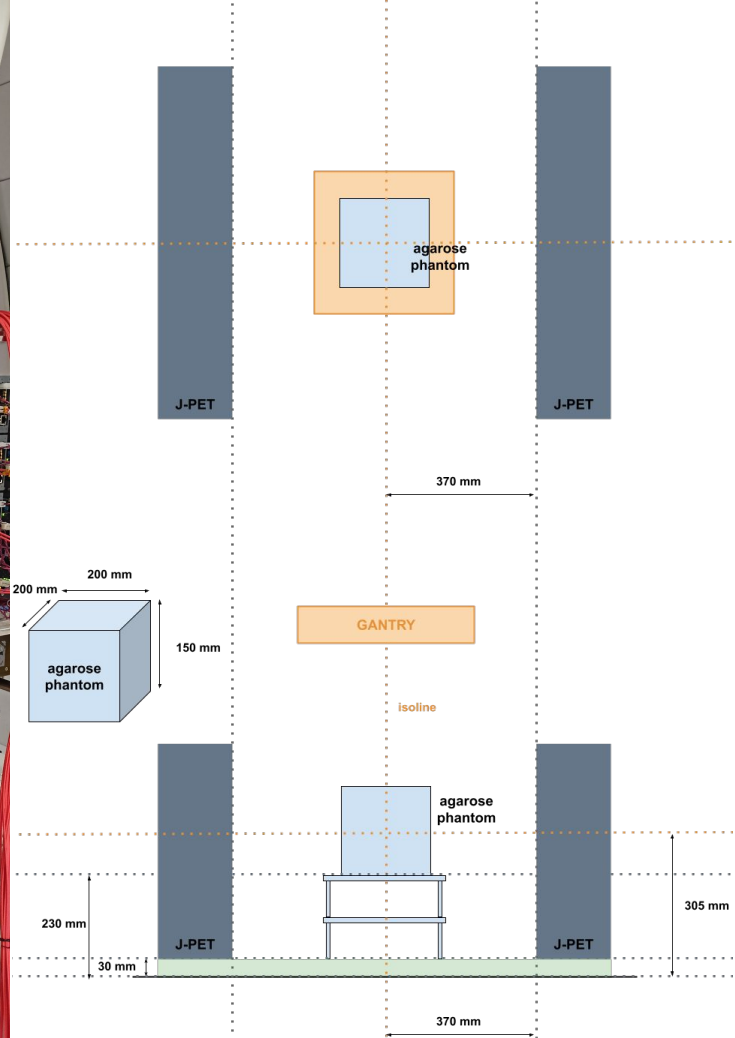
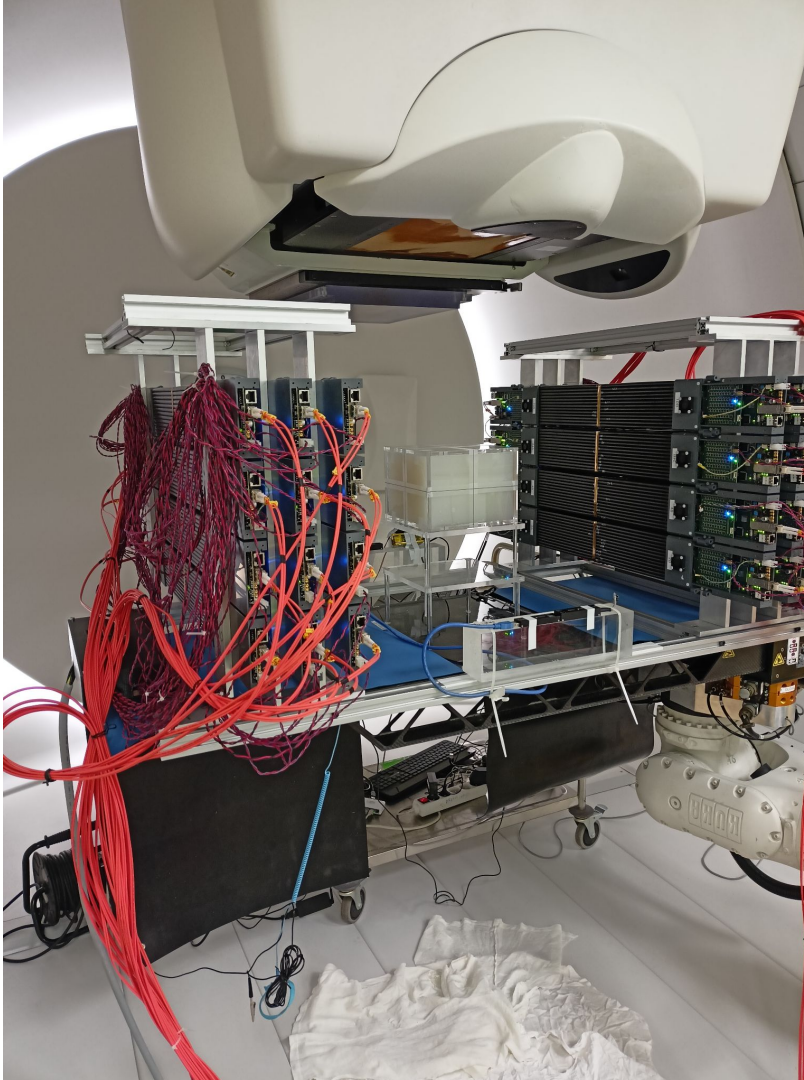


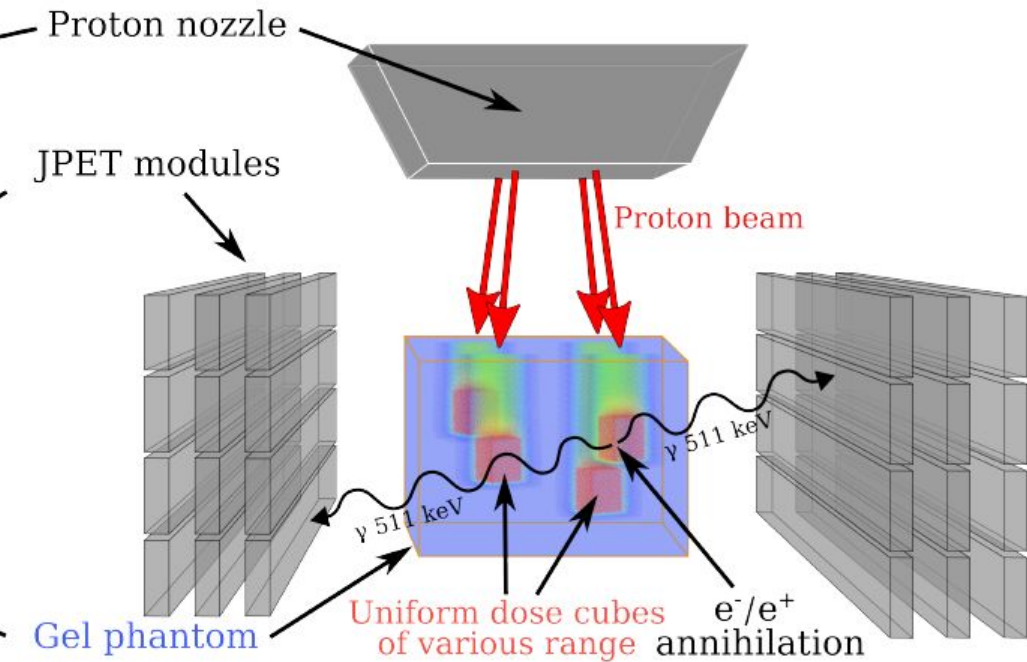
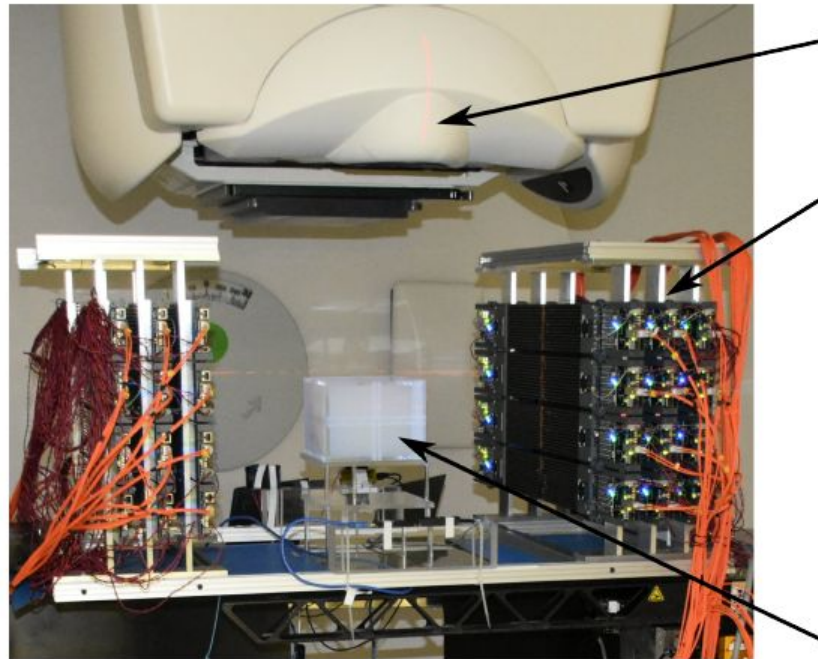
J-PET modular configuration

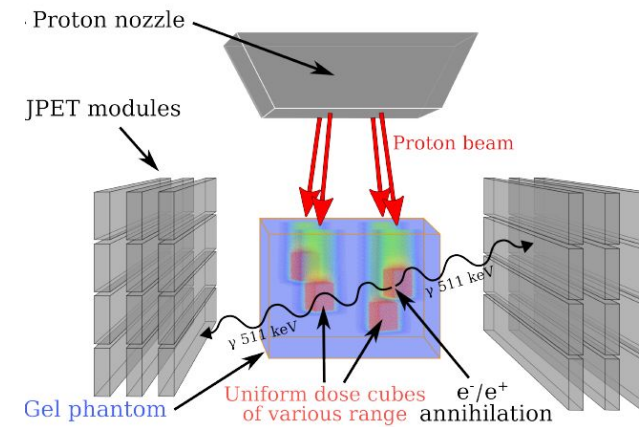


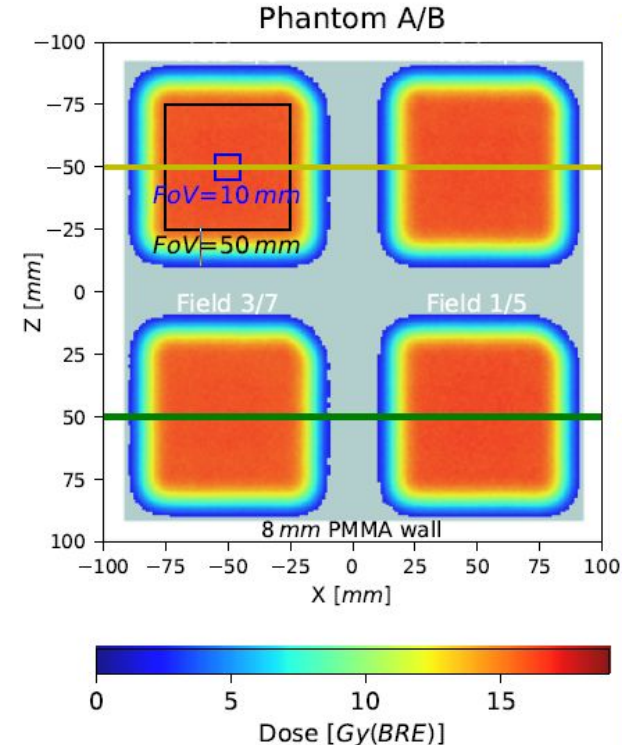
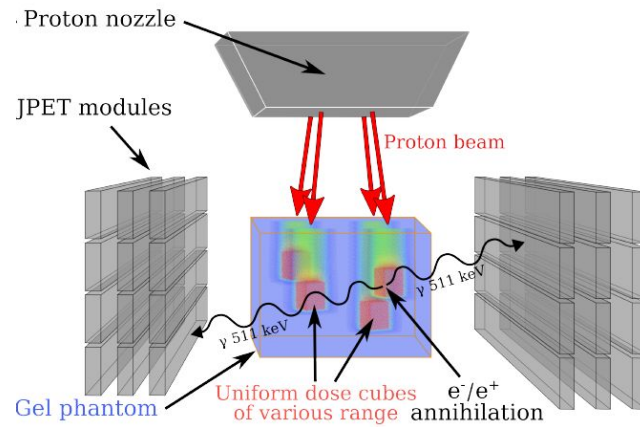


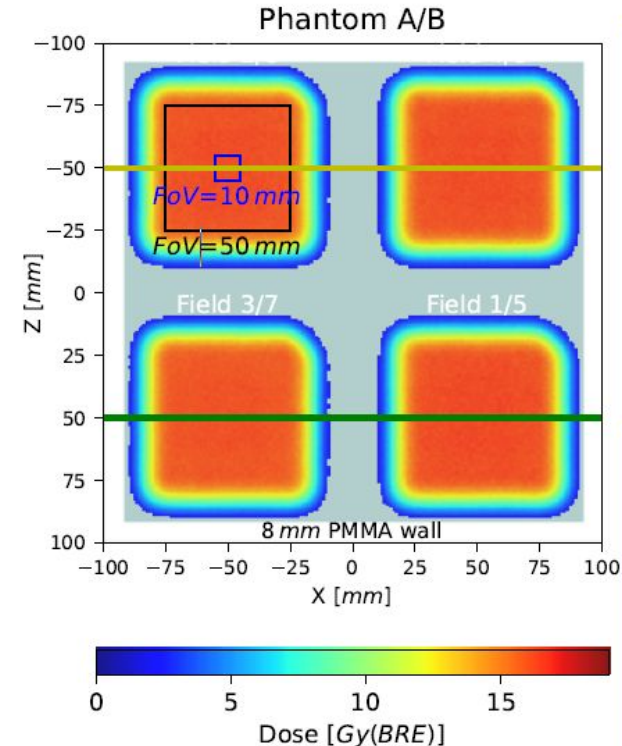
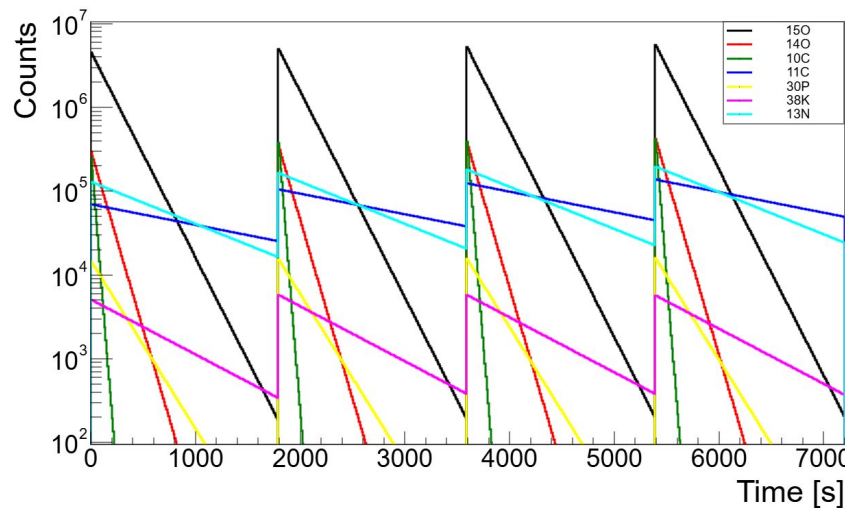
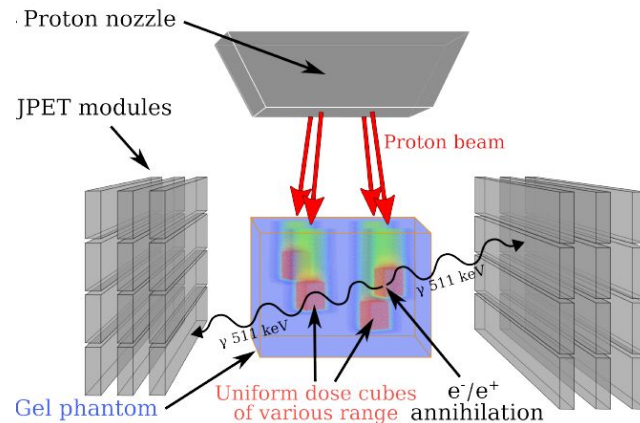
Magdalena Kłodowska. "Application of Monte Carlo methods in transport modelling of the therapeutic proton beam." PhD thesis.
Institute of Nuclear Physics Polish Academy of Science. 2018.

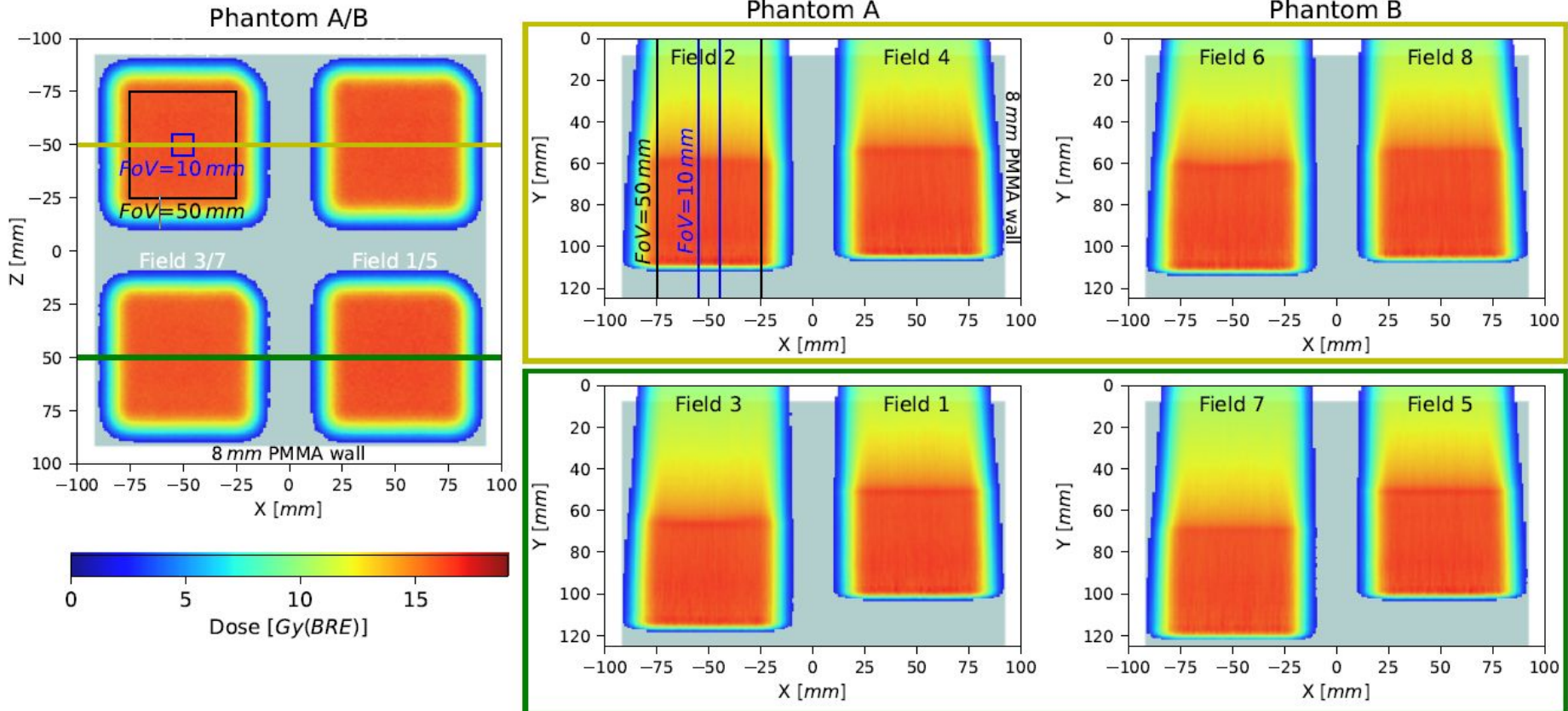




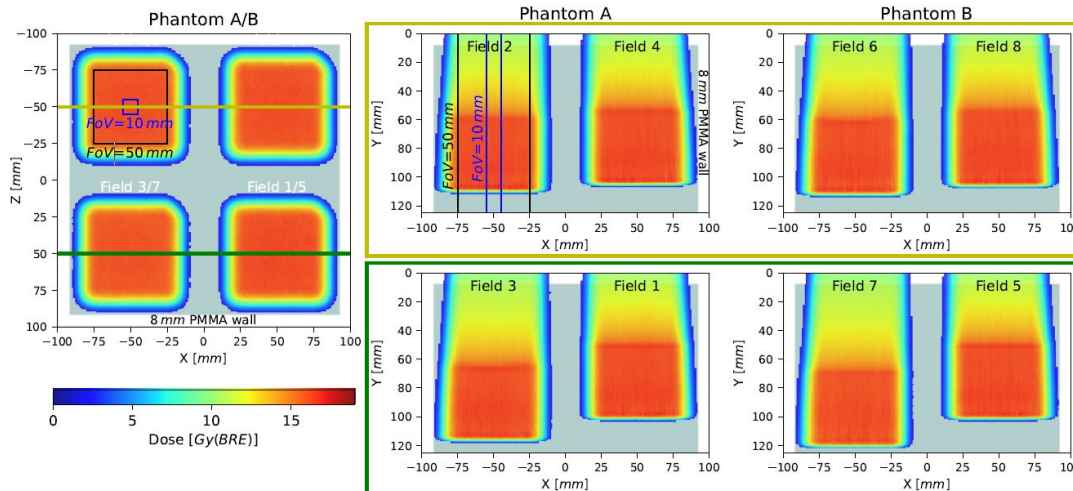




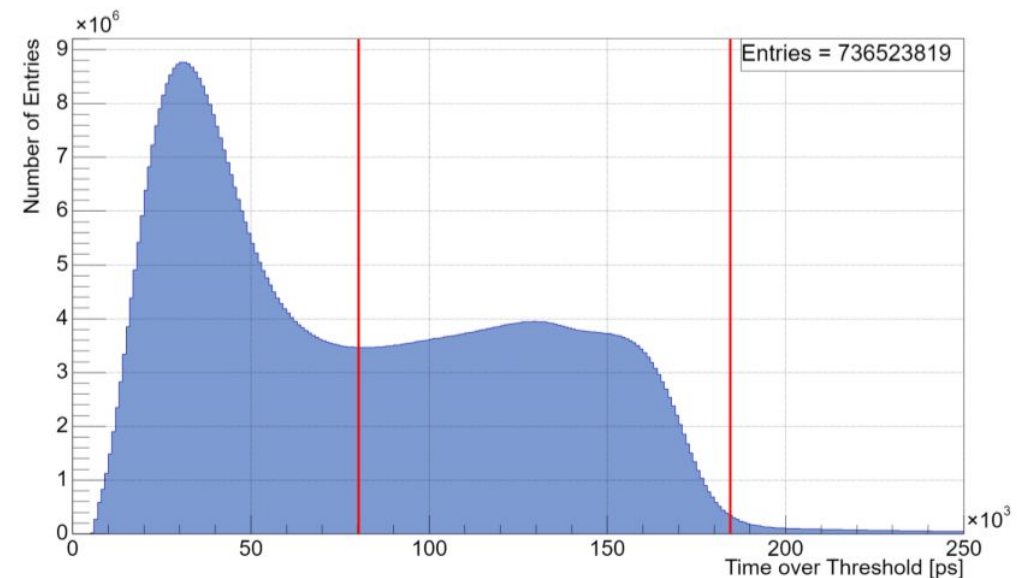
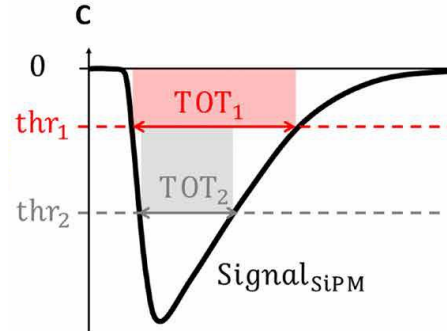




Phantom	Field	Nominal Range [mm]	Range at 50% [mm]	Acquisition time [min]
A	1	100	101.89	30
	2	108	109.98	31
	3	115	116.88	29
	4	103	105.10	30
B	5	100	101.88	33
	6	110	112.10	32
	7	119	121.19	32
	8	104	106.17	35

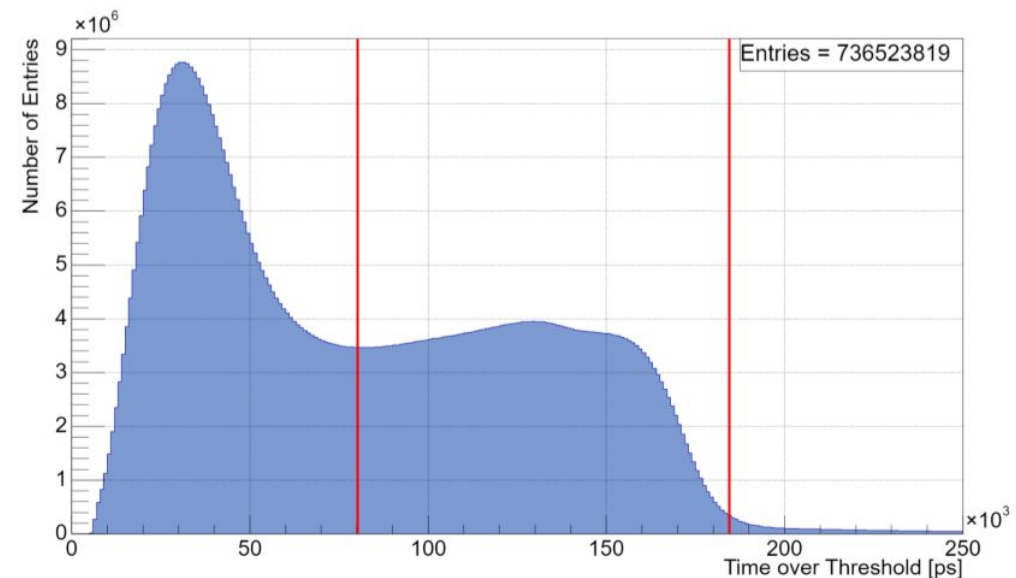
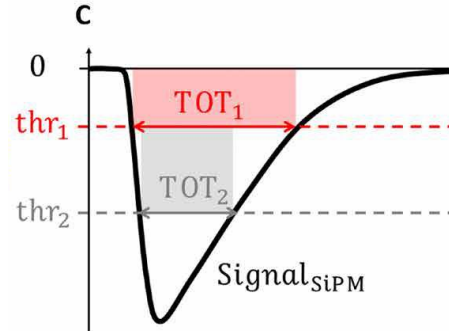


Data selection



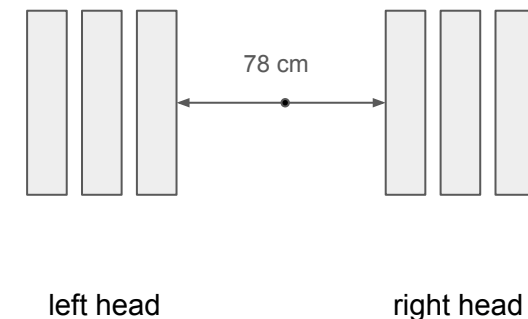
Data selection:

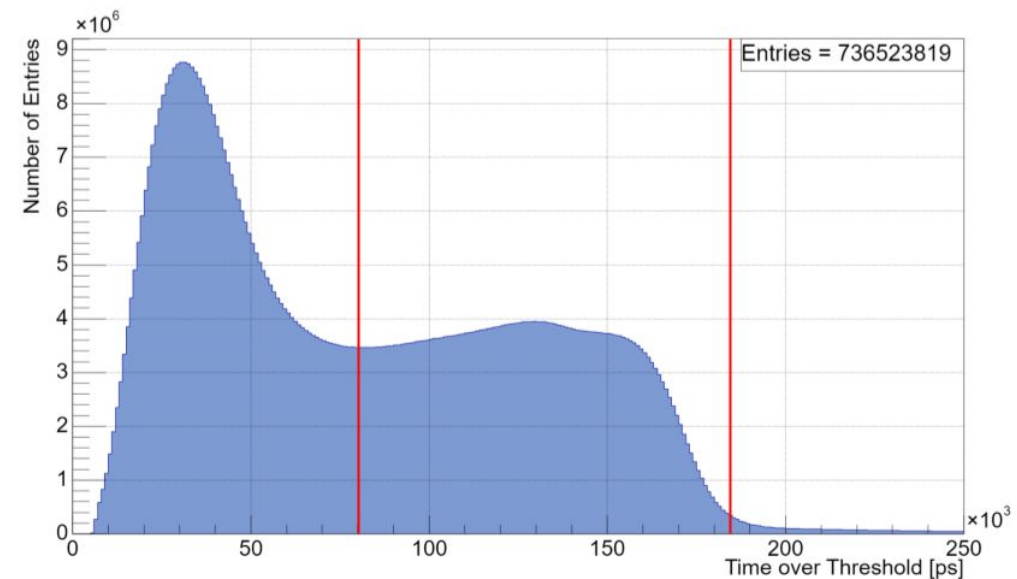
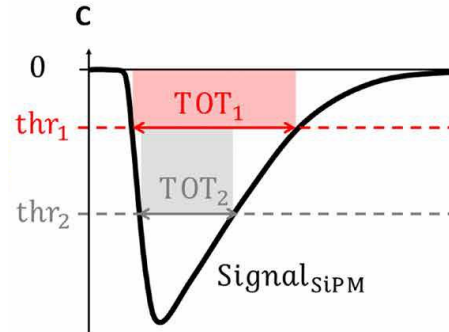
- **unscattered
annihilation gamma
quanta**
- only two interactions
each within different
head
- annihilation point within
system FOV
- scatter test > 40 cm



Data selection:

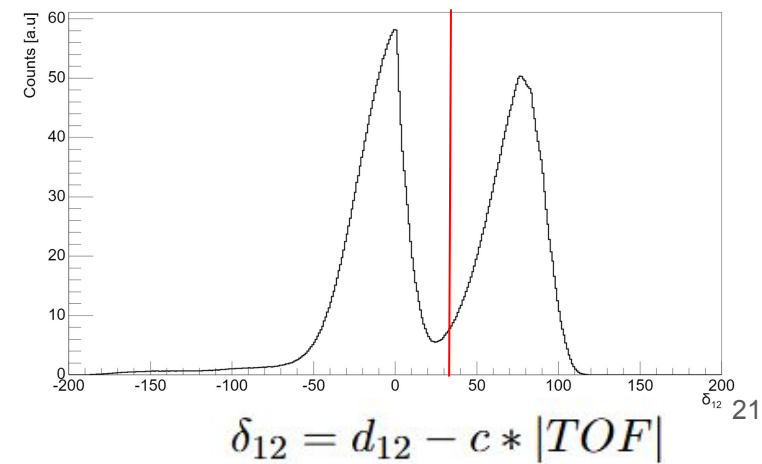
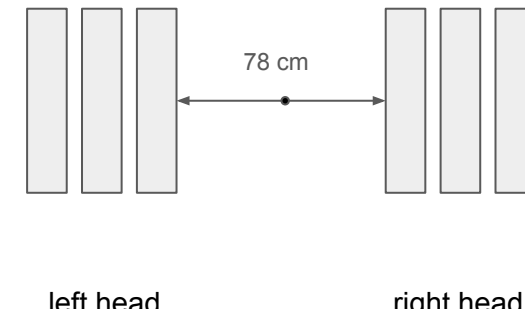
- unscattered annihilation gamma quanta
- **only two interactions each within different head**
- **annihilation point within system FOV**
- scatter test > 40 cm





Data selection:

- unscattered annihilation gamma quanta
- only two interactions each within different head
- annihilation point within system FOV
- **scatter test > 40 cm**

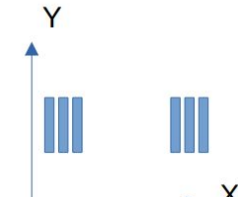
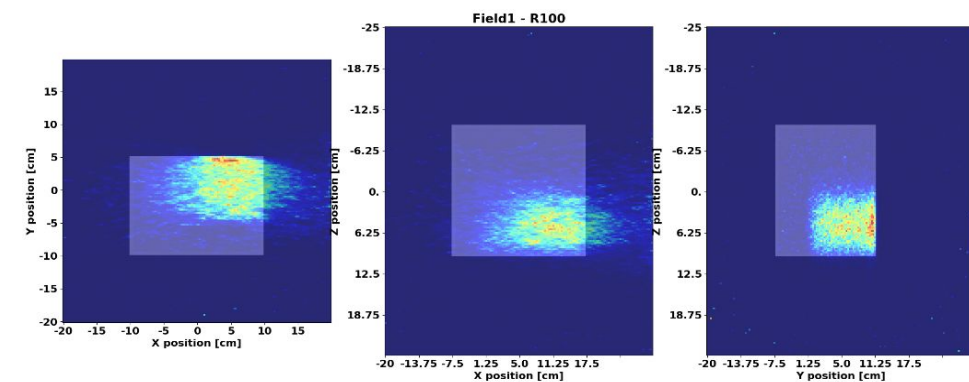


$$\delta_{12} = d_{12} - c * |TOF|$$

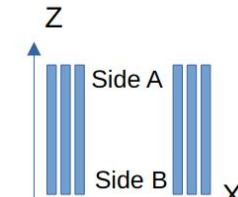
Reconstruction

For the J-PET data reconstruction, the CASToR software has been used with following settings:

- TOF LM-MLEM (5 iterations) with TOF=600 ps
- Ray-tracing Siddon projector (10 rays)
- Attenuation and sensitivity corrections incorporated
- All (true, scatter, random) coincidences taken into account
- No additional PSF modeling added

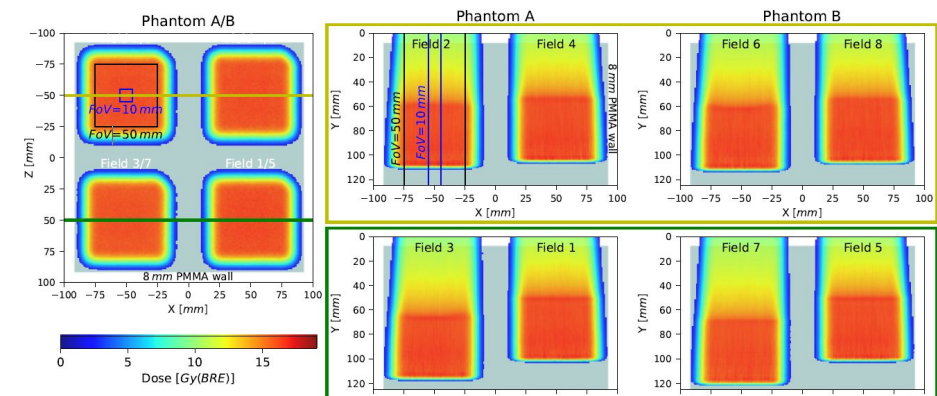
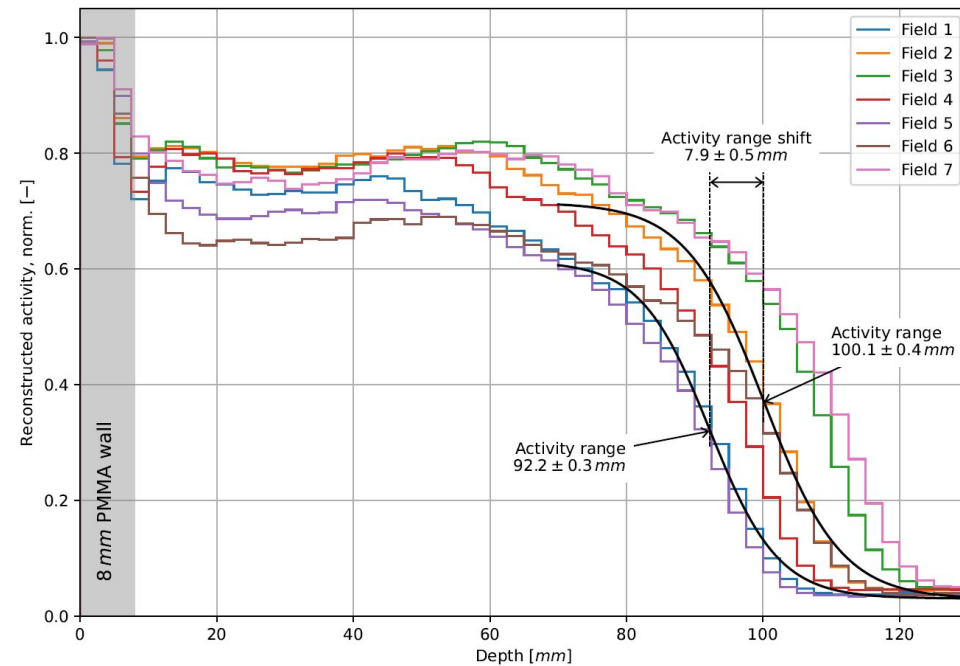


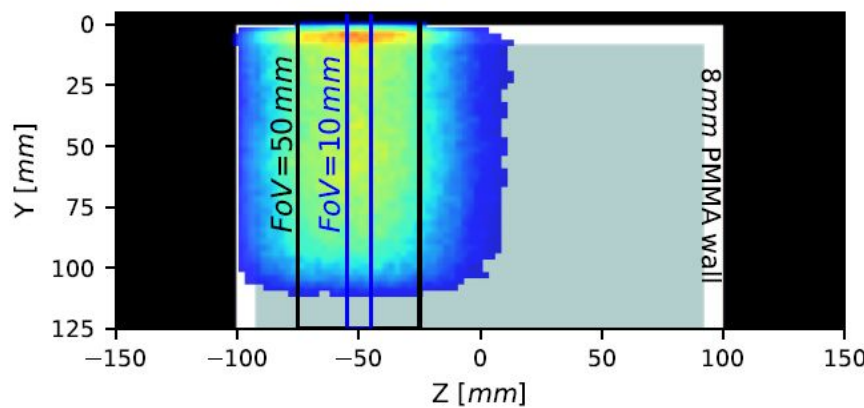
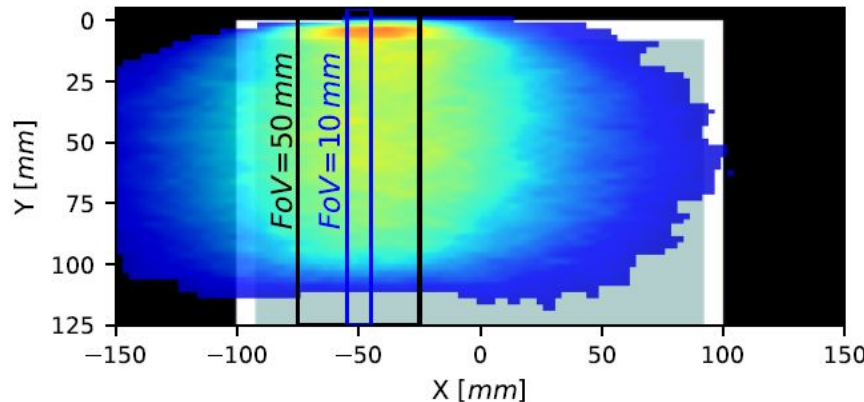
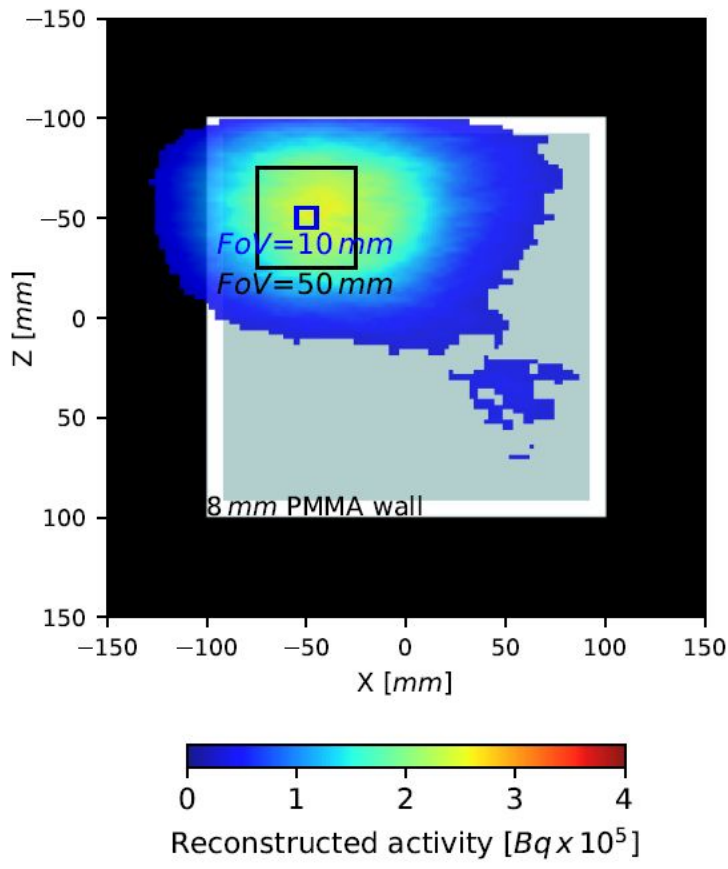
Front view from side B



View from the top

Determination of activity shifts





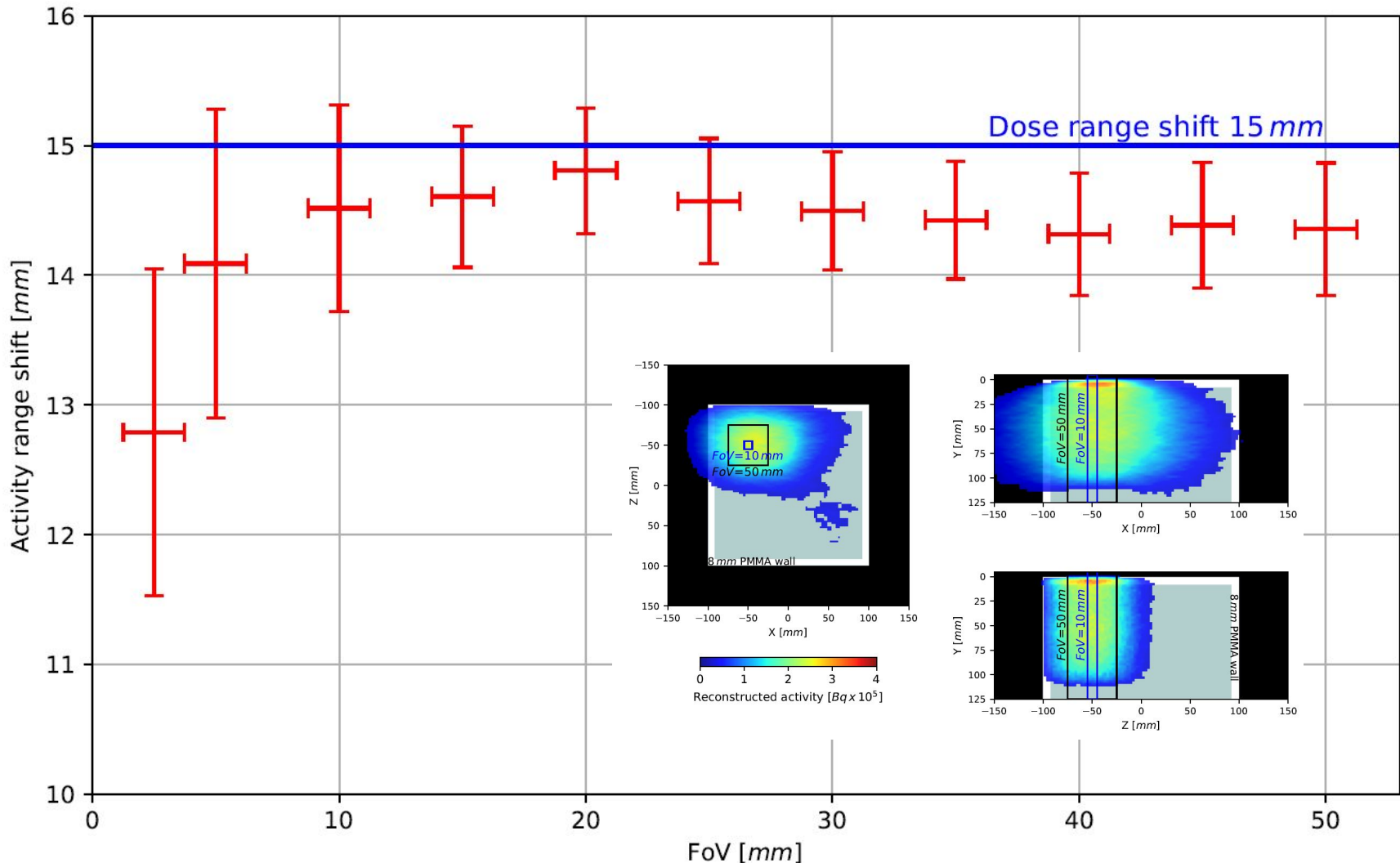
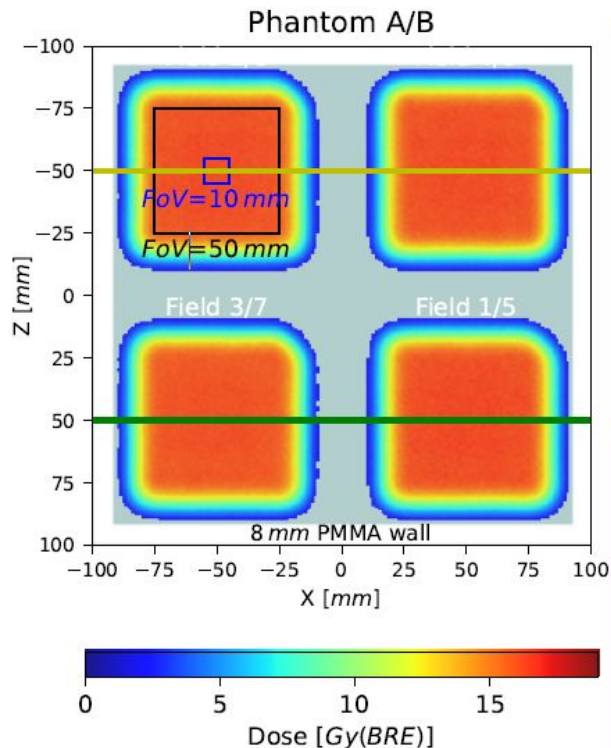


Illustration of all possible combinations:



Phantom	Field	Nominal Range [mm]	Range at 50% [mm]	Acquisition time [min]
A	1	100	101.89	30
	2	108	109.98	31
	3	115	116.88	29
	4	103	105.10	30
B	5	100	101.88	33
	6	110	112.10	32
	7	119	121.19	32
	8	104	106.17	35

Phantom A

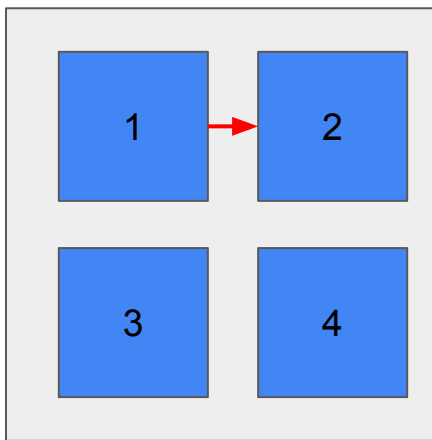
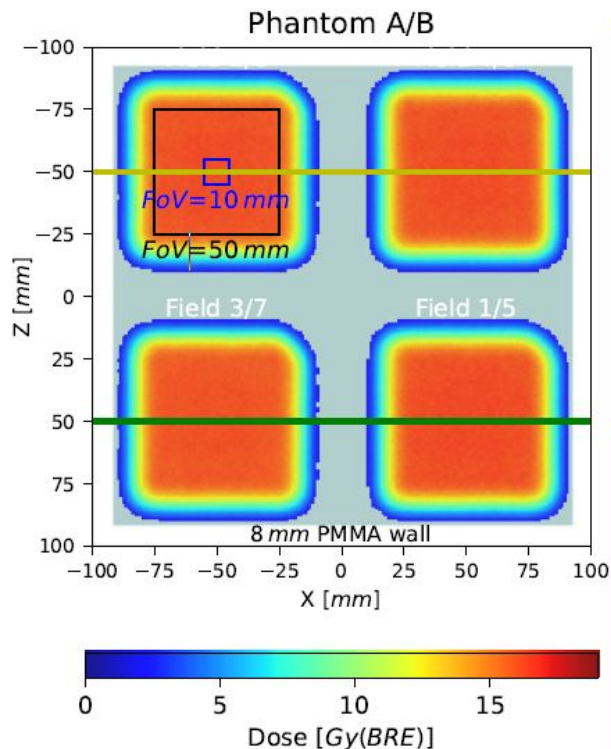


Illustration of all possible combinations:



Phantom	Field	Nominal Range [mm]	Range at 50% [mm]	Acquisition time [min]
A	1	100	101.89	30
	2	108	109.98	31
	3	115	116.88	29
	4	103	105.10	30
B	5	100	101.88	33
	6	110	112.10	32
	7	119	121.19	32
	8	104	106.17	35

Phantom A

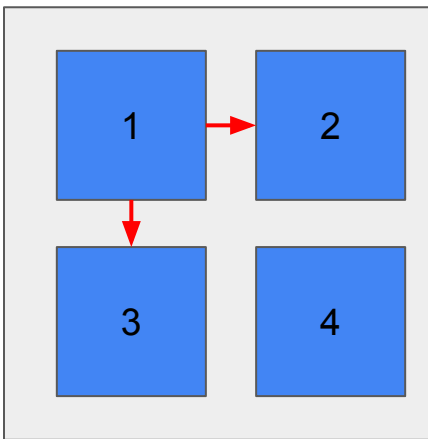
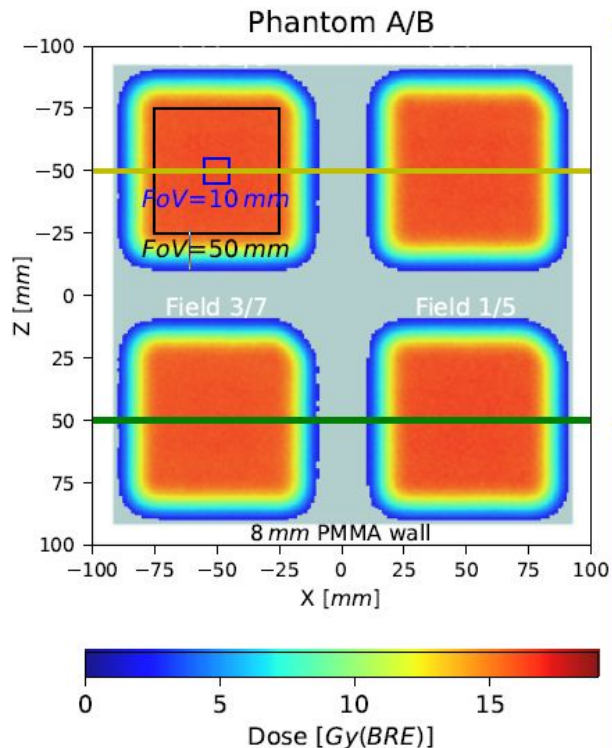


Illustration of all possible combinations:



Phantom	Field	Nominal Range [mm]	Range at 50% [mm]	Acquisition time [min]
A	1	100	101.89	30
	2	108	109.98	31
	3	115	116.88	29
	4	103	105.10	30
B	5	100	101.88	33
	6	110	112.10	32
	7	119	121.19	32
	8	104	106.17	35

Phantom A

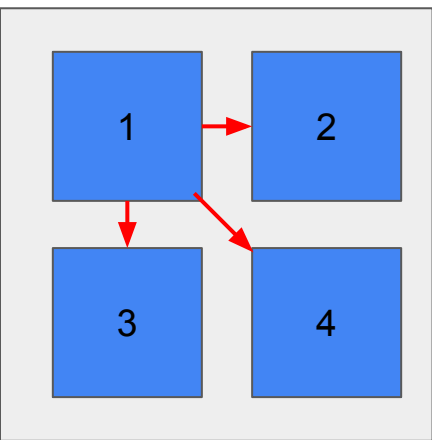
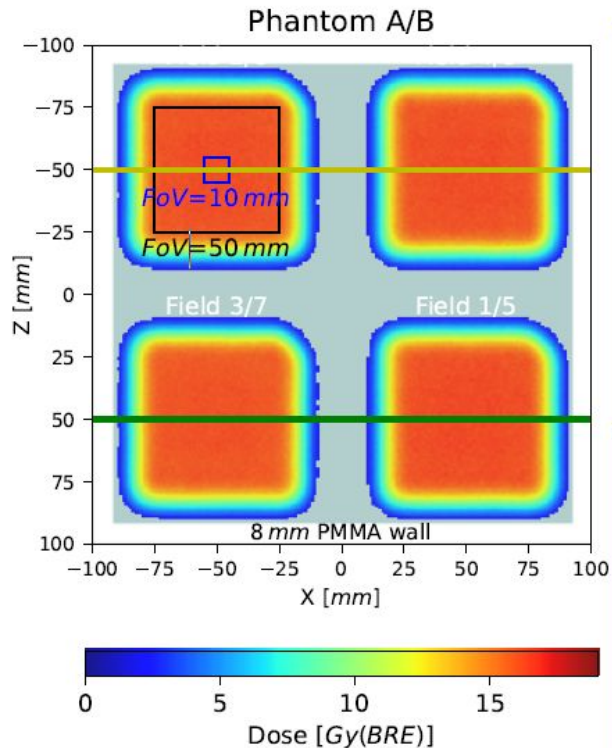
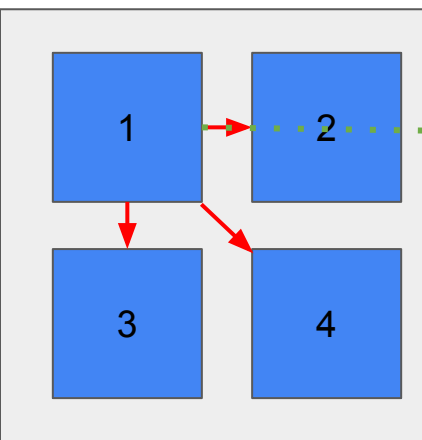


Illustration of all possible combinations:



Phantom	Field	Nominal Range [mm]	Range at 50% [mm]	Acquisition time [min]
A	1	100	101.89	30
	2	108	109.98	31
	3	115	116.88	29
	4	103	105.10	30
B	5	100	101.88	33
	6	110	112.10	32
	7	119	121.19	32
	8	104	106.17	35

Phantom A



Phantom B

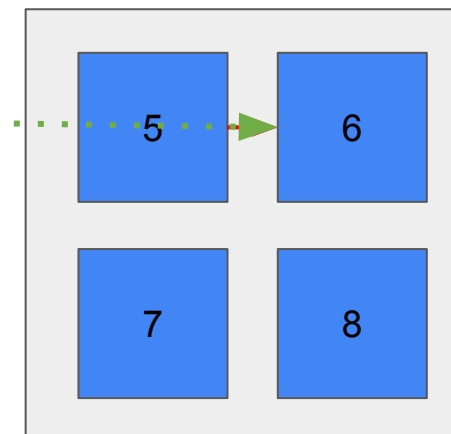
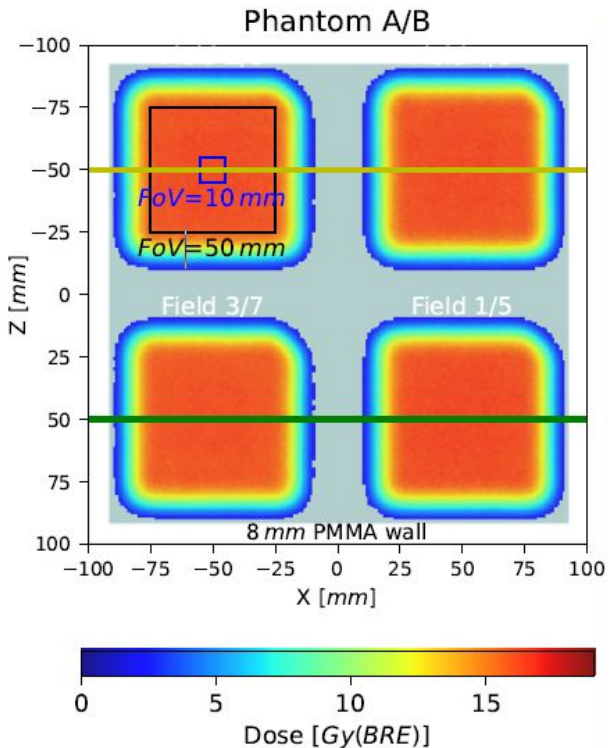
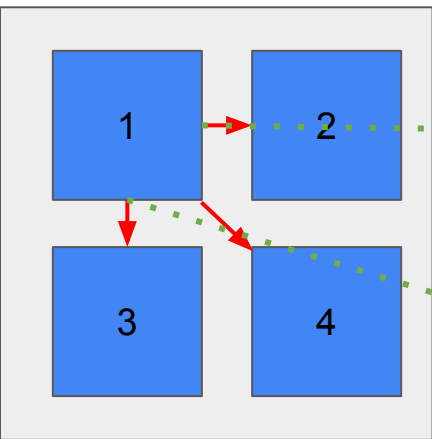


Illustration of all possible combinations:

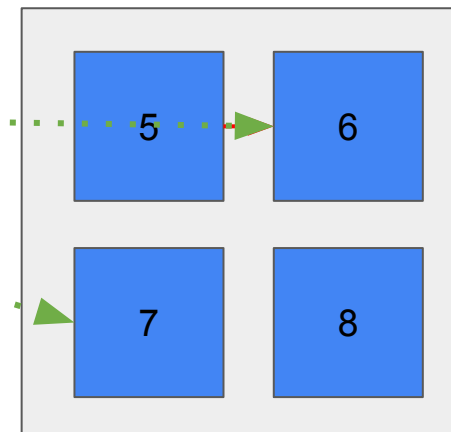


Phantom	Field	Nominal Range [mm]	Range at 50% [mm]	Acquisition time [min]
A	1	100	101.89	30
	2	108	109.98	31
	3	115	116.88	29
	4	103	105.10	30
B	5	100	101.88	33
	6	110	112.10	32
	7	119	121.19	32
	8	104	106.17	35

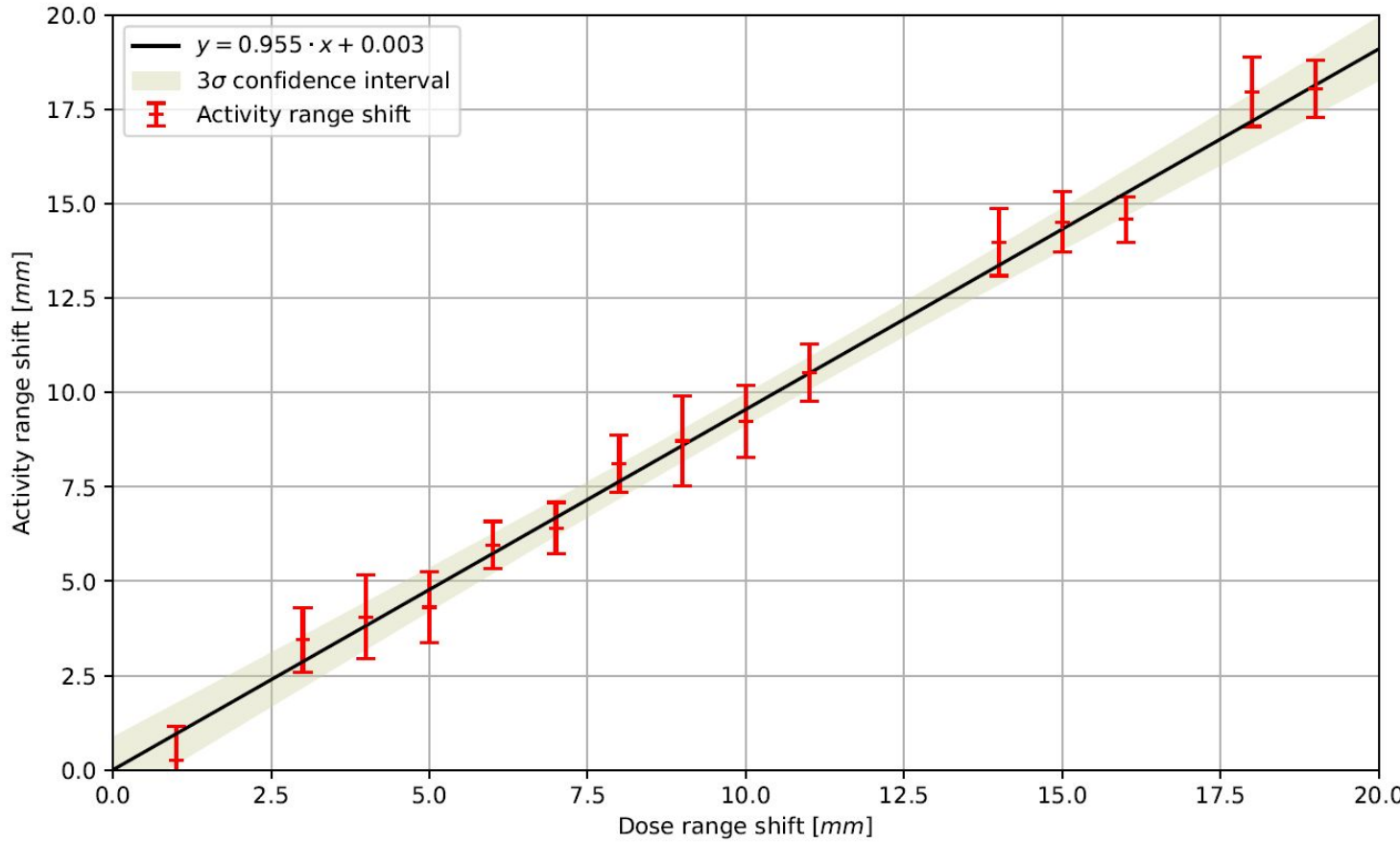
Phantom A

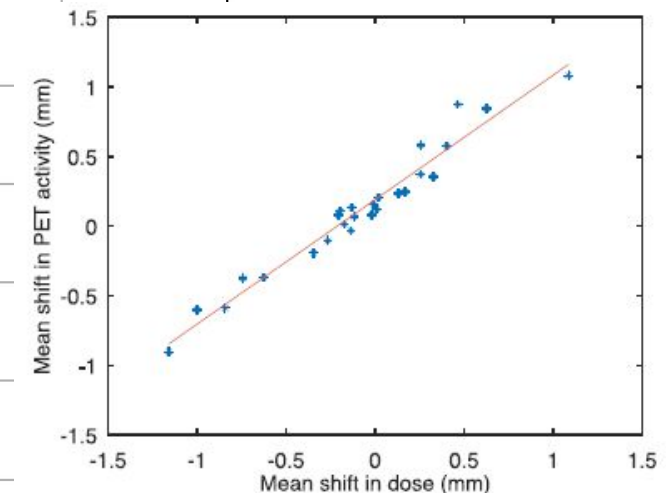
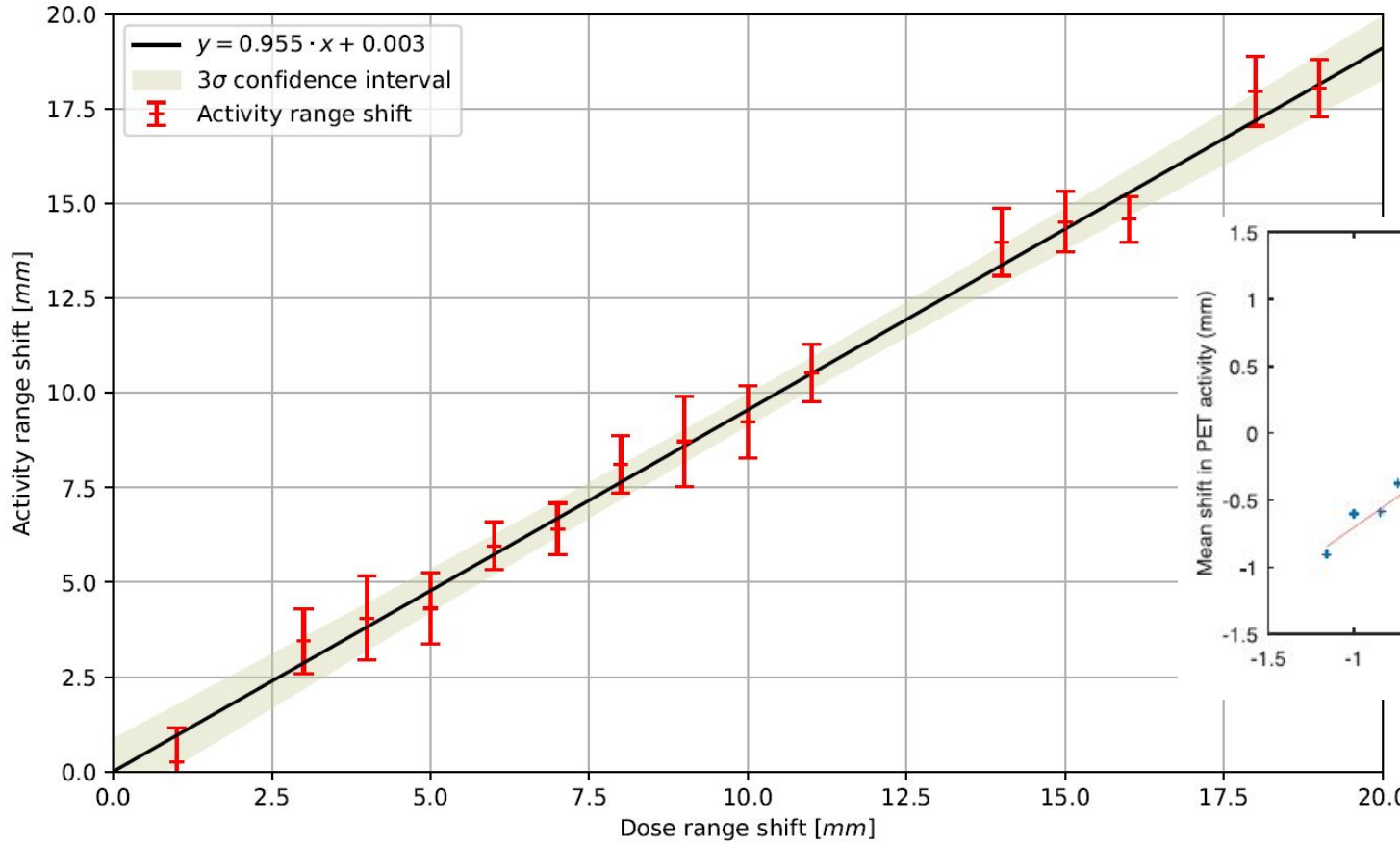


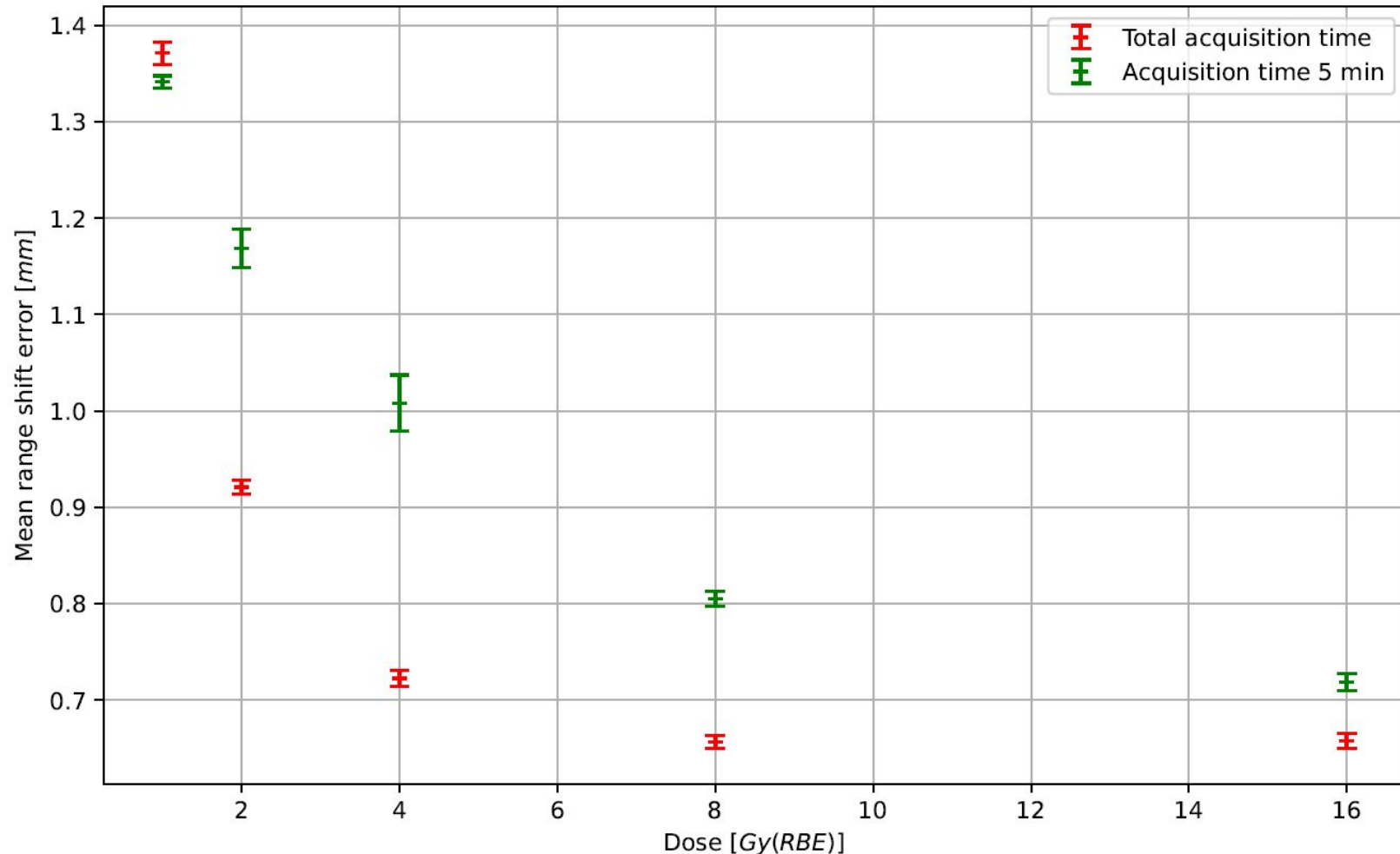
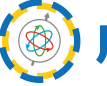
Phantom B



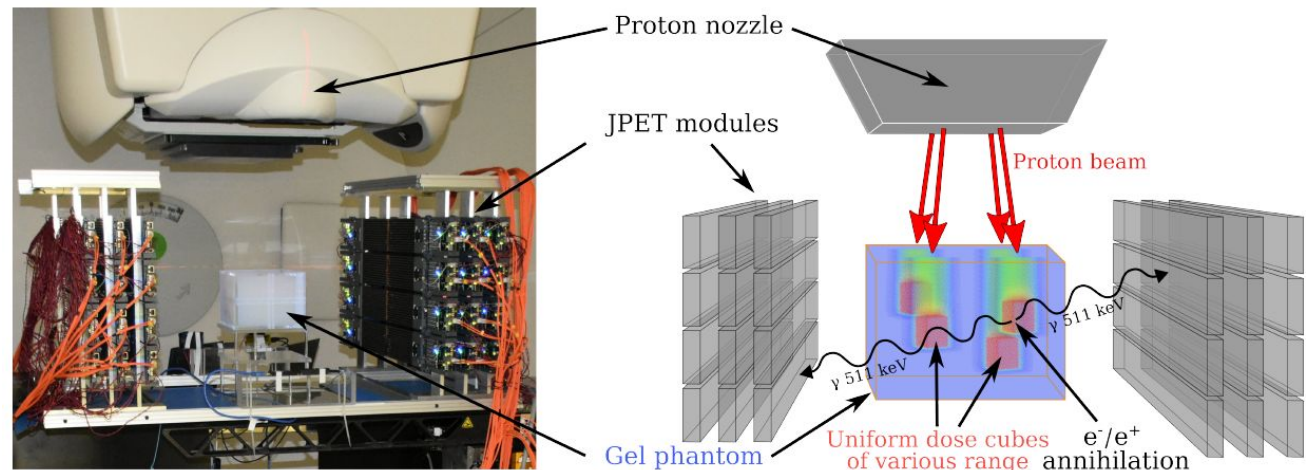
Results



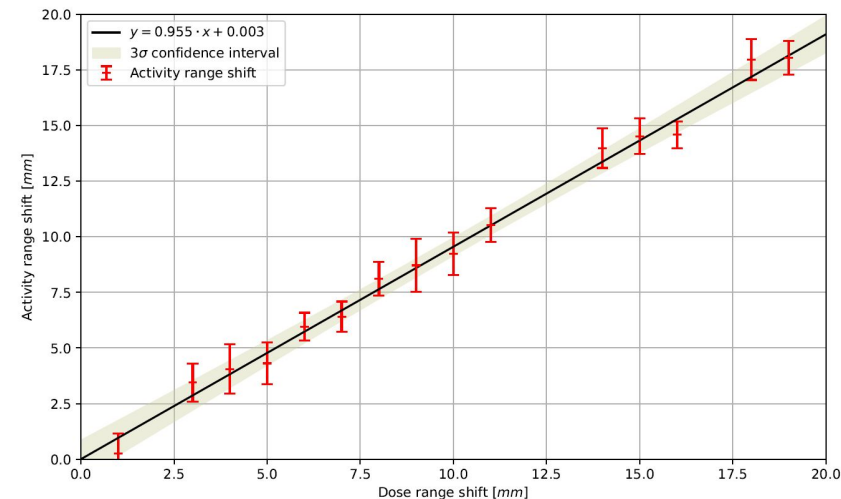




Summary



- we have successfully determined proton range shifts in agarous phantoms with modular J-PET
- a linear dependence between dose and activity shifts was observed
- after system upgrade an on-beam measurements will be possible



Thank you for your attention

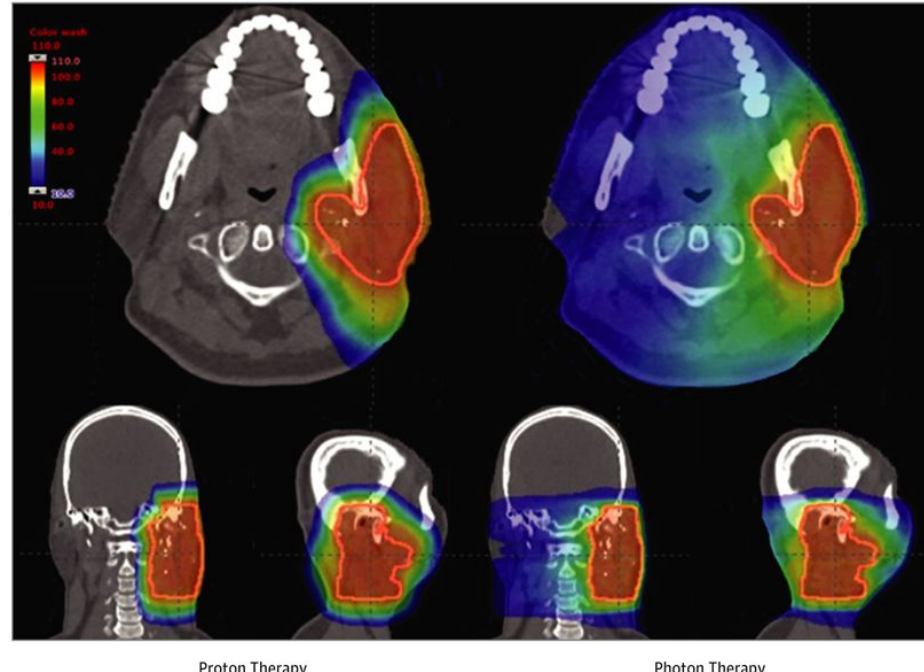


Paweł Moskal, Grzegorz Korcyl, Maciej Bakalarek, Damian Borys, Antoni Ruciński, Jan Gajewski, Karol Brzeziński, Jakub Baran, Paulina Stasica et al.

Backup

Proton therapy

- Pediatric tumors: reduced late toxicity and secondary malignancy risk.
- Head & neck, skull-base tumors: improved sparing of salivary glands/brainstem.
- Ocular and selected CNS tumors: excellent local control.
- Some studies show comparable tumor control to photons.



Baumann BC, Mitra N, Harton JG, et al. Comparative Effectiveness of Proton vs Photon Therapy as Part of Concurrent Chemoradiotherapy for Locally Advanced Cancer. JAMA Oncol. 2020;6(2):237–246. doi:10.1001/jamaoncol.2019.4889

Chen Z, et al. Proton versus photon radiation therapy: A clinical review. Front Oncol. 2023 Mar 29;13:1133909. doi: 10.3389/fonc.2023.1133909

Efstathiou, J.A. et al., Prostate Advanced Radiation Technologies Investigating Quality of Life (PARTIQoL): Phase III Randomized Clinical Trial of Proton Therapy vs. IMRT for Localized Prostate Cancer International Journal of Radiation Oncology, Biology, Physics, Volume 120, Issue 2, S1 October 01, 2024.

Proton range determination

1. Dual-energy CT (DECT) / photon-counting CT (PCCT)

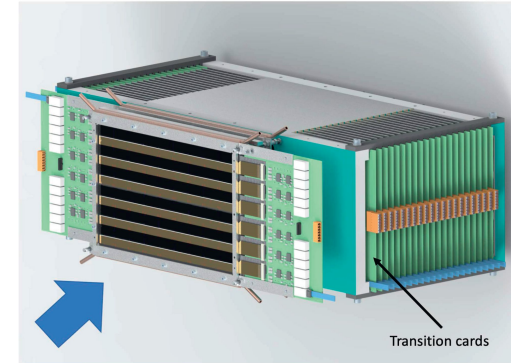
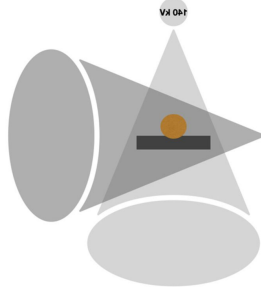
Charles Ekene Chika, World J Radiol. 2025 Jun 28;17(6):105728. doi: 10.4329/wjr.v17.i6.105728

2. Proton CT (pCT) / proton radiography (pRad)

Alme J, et al.(2020) A High-Granularity Digital Tracking Calorimeter Optimized for Proton CT. Front. Phys. 8:568243. doi: 10.3389/fphy.2020.568243

3. Machine learning & Monte-Carlo aid

Wildman VL, et al.. Recent advances in applying machine learning to proton radiotherapy. Biomed Phys Eng Express. 2025 Jul 23;11(4):042005. doi: 10.1088/2057-1976/adeb90. PMID: 40609552; PMCID: PMC12284894.



Main sources of uncertainty:

- morphological changes,
- anatomical deformation due to motion
- HU to RSP conversion error

1. Prompt Gamma Imaging (PGI) / Prompt Gamma Spectroscopy (PGS) / Prompt Gamma Timing (PGT)

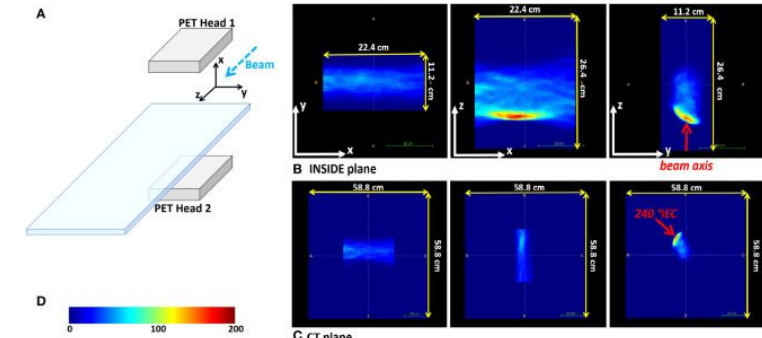
Everaere P, et al. Prompt gamma energy integration: a new method for online-range verification in proton therapy with pulsed-beams. Front. Phys. 12:1371015. doi: 10.3389/fphy.2024.1371015

2. Ionoacoustic / protoacoustic imaging

Alme J, et Wang S, et al. Real-time tracking of the Bragg peak during proton therapy via 3D protoacoustic Imaging in a clinical scenario. Npj Imaging. 2024;2(1):34. doi: 10.1038/s44303-024-00039-x. Epub 2024 Sep 17. PMID: 40078731; PMCID: PMC11893450.

3. In-beam PET and delayed gamma imaging

Moglionico M, et al. In-vivo range verification analysis with in-beam PET data for patients treated with proton therapy at CNAO. Front Oncol. 2022 Sep 26;12:929949. doi: 10.3389/fonc.2022.929949. PMID: 36226070; PMCID: PMC9549776.



PAPER

Detection of range shifts in proton beam therapy using the J-PET scanner: a patient simulation study

Karol Brzeziński^{1,2,*}, Jakub Baran^{3,4,5}, Damian Borys^{6,7}, Jan Gajewski¹, Neha Chug^{3,4,5}, Aurélien Coussat^{3,4,5}, Eryk Czerwiński^{3,4,5}, Meysam Dadgar^{3,4,5}, Kamil Dulski^{3,4,5}, Kavya V. Eliyan^{3,4,5}, Aleksander Gajos^{3,4,5}, Krzysztof Kapczak^{3,4,5}, Łukasz Kaplon^{3,4,5}, Konrad Klimaszewski³, Paweł Konieczka³, Renata Kopec³, Grzegorz Korczyk^{3,4,5}, Tomasz Kozik^{3,4,5}, Wojciech Krzemień⁹, Deepak Kumar^{4,5}, Antony J. Lomax^{10,11}, Keegan McNamara^{10,11}, Szymon Niedźwiecki^{3,4,5}, Paweł Olko³, Dominik Panek^{3,4,5}, Szymon Parzych^{3,4,5}, Elena Perez del Rio^{3,4,5}, Lech Raczyński¹, Sushil Sharma^{3,4,5}, Shivani^{3,4,5}, Roman Y. Shopa³, Tomasz Skóra¹², Małgorzata Skurzok^{3,4,5}, Paulina Stasica¹⁰, Ewa Ł. Stępien^{3,4,5}, Keyvan Tayefi^{3,4,5}, Faranak Tayefi^{3,4,5}, Damien C. Weber^{10,13,14}, Carla Winterhalter^{10,11}, Wojciech Wiślicki⁸, Paweł Moskal^{3,4,5} and Antoni Ruciński³

Physica Medica 118 (2024) 103301

Contents lists available at ScienceDirect

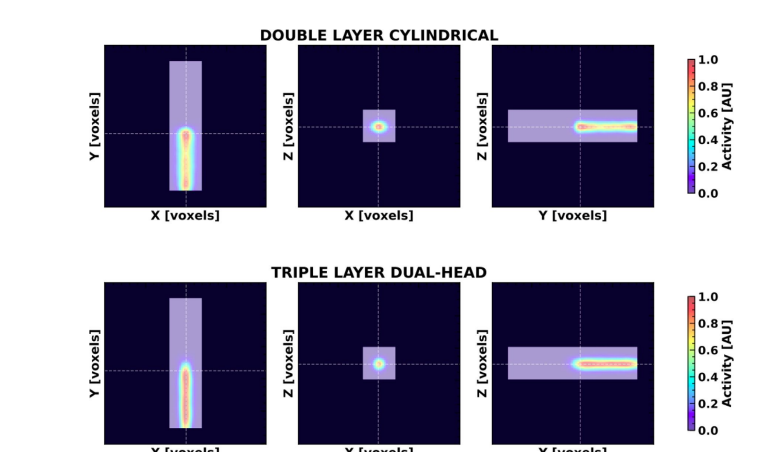
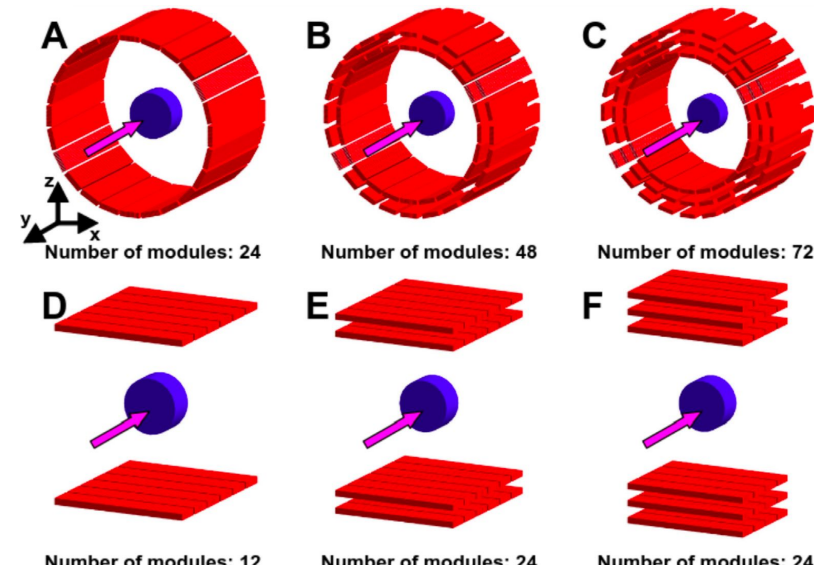
Physica Medica

journal homepage: www.elsevier.com/locate/ejmp

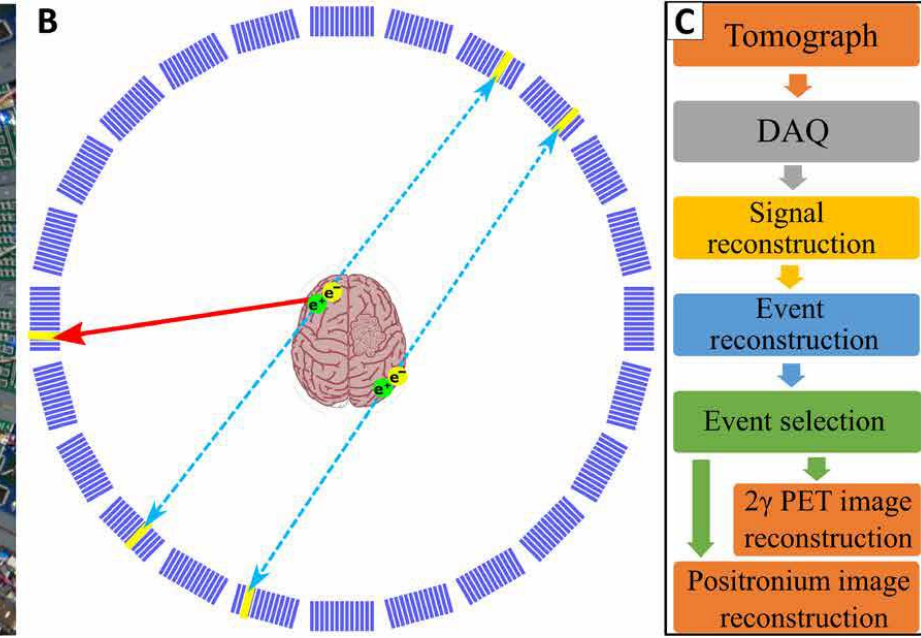
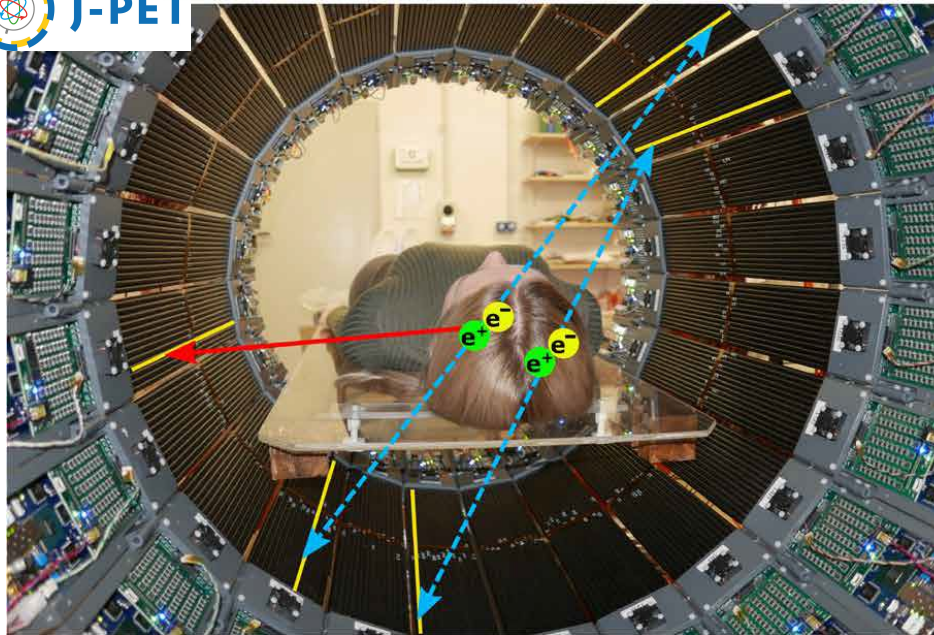
Technical note

Feasibility of the J-PET to monitor the range of therapeutic proton beams

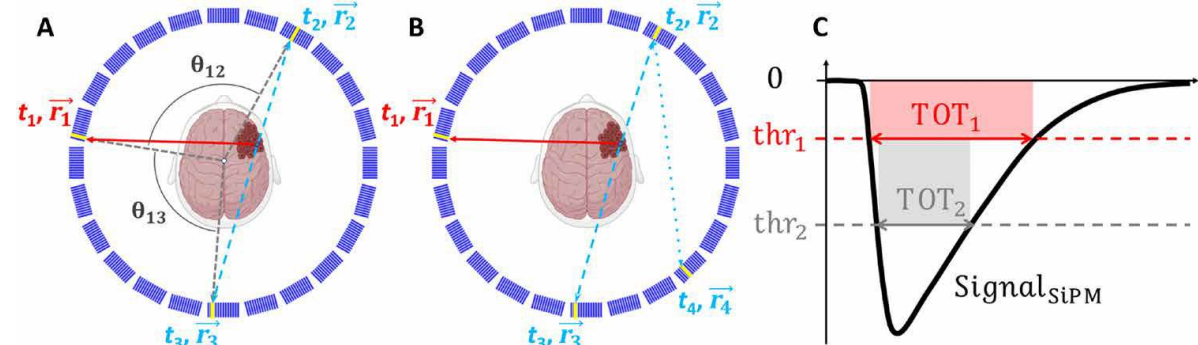
Jakub Baran^{3,4,5,*}, Damian Borys^{3,4,5}, Karol Brzeziński^{1,6}, Jan Gajewski¹, Michał Siliński^{3,4,5}, Neha Chug^{3,4,5}, Aurélien Coussat^{3,4,5}, Eryk Czerwiński^{3,4,5}, Meysam Dadgar^{3,4,5}, Kamil Dulski^{3,4,5}, Kavya V. Eliyan^{3,4,5}, Aleksander Gajos^{3,4,5}, Krzysztof Kapczak^{3,4,5}, Łukasz Kaplon^{3,4,5}, Konrad Klimaszewski³, Paweł Konieczka³, Renata Kopec³, Grzegorz Korczyk^{3,4,5}, Tomasz Kozik^{3,4,5}, Wojciech Krzemień⁹, Deepak Kumar^{4,5}, Antony J. Lomax^{10,11}, Keegan McNamara^{10,11}, Szymon Niedźwiecki^{3,4,5}, Paweł Olko³, Dominik Panek^{3,4,5}, Szymon Parzych^{3,4,5}, Elena Perez del Rio^{3,4,5}, Lech Raczyński¹, Moyo Simbarashe^{3,4,5}, Sushil Sharma^{3,4,5}, Shivani^{3,4,5}, Roman Y. Shopa³, Tomasz Skóra¹², Małgorzata Skurzok^{3,4,5}, Paulina Stasica¹⁰, Ewa Ł. Stępien^{3,4,5}, Keyvan Tayefi^{3,4,5}, Faranak Tayefi^{3,4,5}, Damien C. Weber^{10,13,14}, Carla Winterhalter^{10,11}, Wojciech Wiślicki⁸, Paweł Moskal^{3,4,5}, Antoni Ruciński³

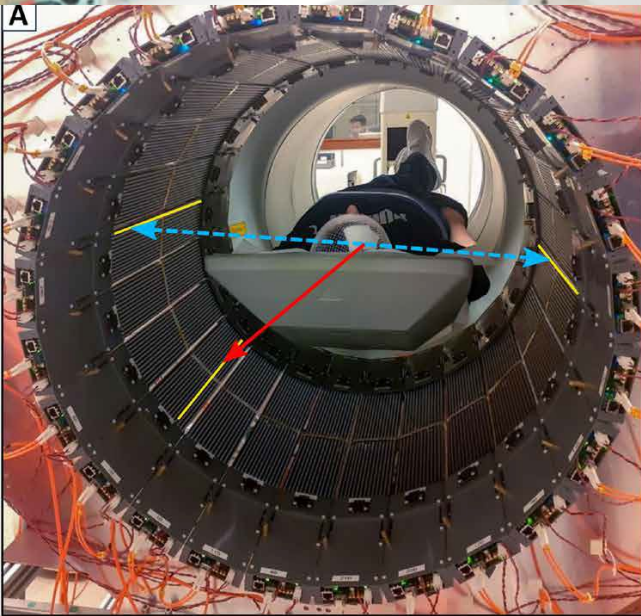


J-PET modular - general



- **modular design**
- 24 modules
- 13 scintillators per module
- 4 SiPM per scintillator side
- 2 constant threshold per SiPM
- 50 cm FOV
- digital data at the module output
- 74 cm diameter
- very light ~60 kg





	Modular J-PET	Total Body uExplorer	PENPET Explorer	Biograph Vision Quadra
Company/facility	Jagellonian University, J-PET group	UC Davis and United Imaging Healthcare	UPenn, KAGE Medical and Philips	Siemens Healthineers, Turku PET
Scintillator type	BC-404	LSO (18.1 mm)	LYSO (19mm)	LSO (20 mm)
Light sensor	MPPC-1X4CH-ARRAY S13361-6674	SensL J-series	Philips Digital Photon Counting	MRD 85
Type of light sensor	Analog	Analog	Digital	Analog
Scintillator cross section (mm^2)	24×6	2.76×2.76	3.86×3.86	3.2×3.2
Axial length (cm)	50	194	64	106
Diameter (cm)	73.9	74	76.4	82
No. of modules	24	-	18	38
No. of rings	1	-	3	32
Time window (ns)	4	4.5-6.9	4	4.7
Energy window (keV)	> 200	430-645	440-600	435 - 585
Sensitivity in center (cps/kBq)	2.1	174	54	82.6
Sensitivity in 10 cm offset from center(cps/kBq)	1.8	177	57	84.1
Scatter fraction (%)	41.68 ± 0.19	36.3	32	37
Radial FWHM (mm)	4.9 ± 0.2	3.0	3.9 ± 0.4	3.19
Tangential FWHM (mm)	7.3 ± 0.1	3.0	3.9 ± 0.4	3.58
Axial FWHM (mm)	30.10 ± 0.01	2.8	4.1 ± 0.2	3.78

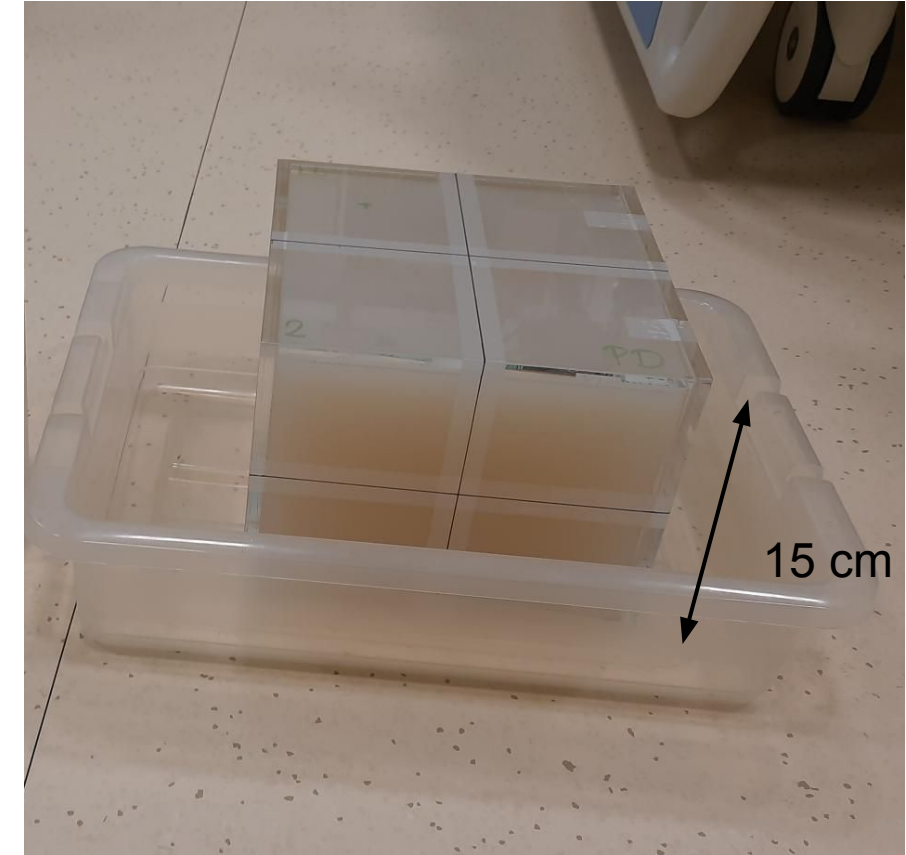
CCB and phantoms

- The Cyclotron Centre Bronowice (CCB) produces and accelerates protons to therapeutic energies from 70 to 230 MeV using the isochronous cyclotron C-230 (IBA, Belgium).
- In Poland, proton therapy is used clinically for radiation therapy at Cyclotron Centre Bronowice (CCB), Krakow Proton Beam Therapy Center of the Institute of Nuclear Physics PAS (IFJ PAS) to treat patients from Krakow and neighboring oncology hospitals, where over 1500 patients have been treated so far.

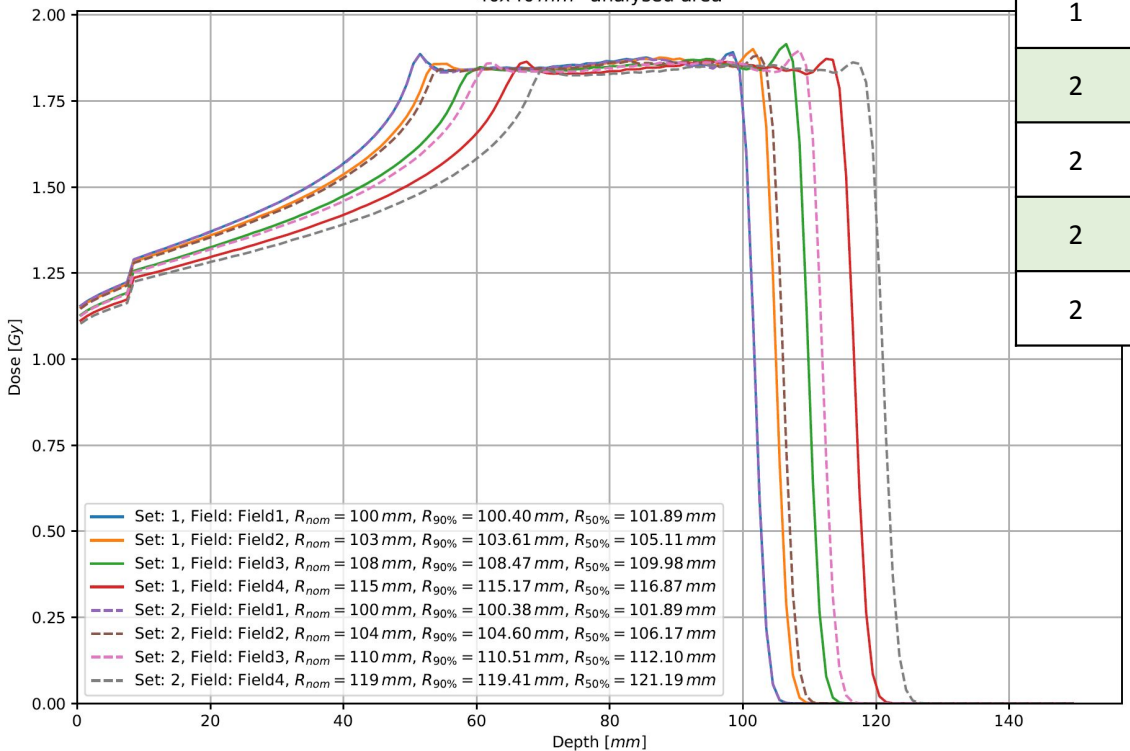


Agarose gel phantom:

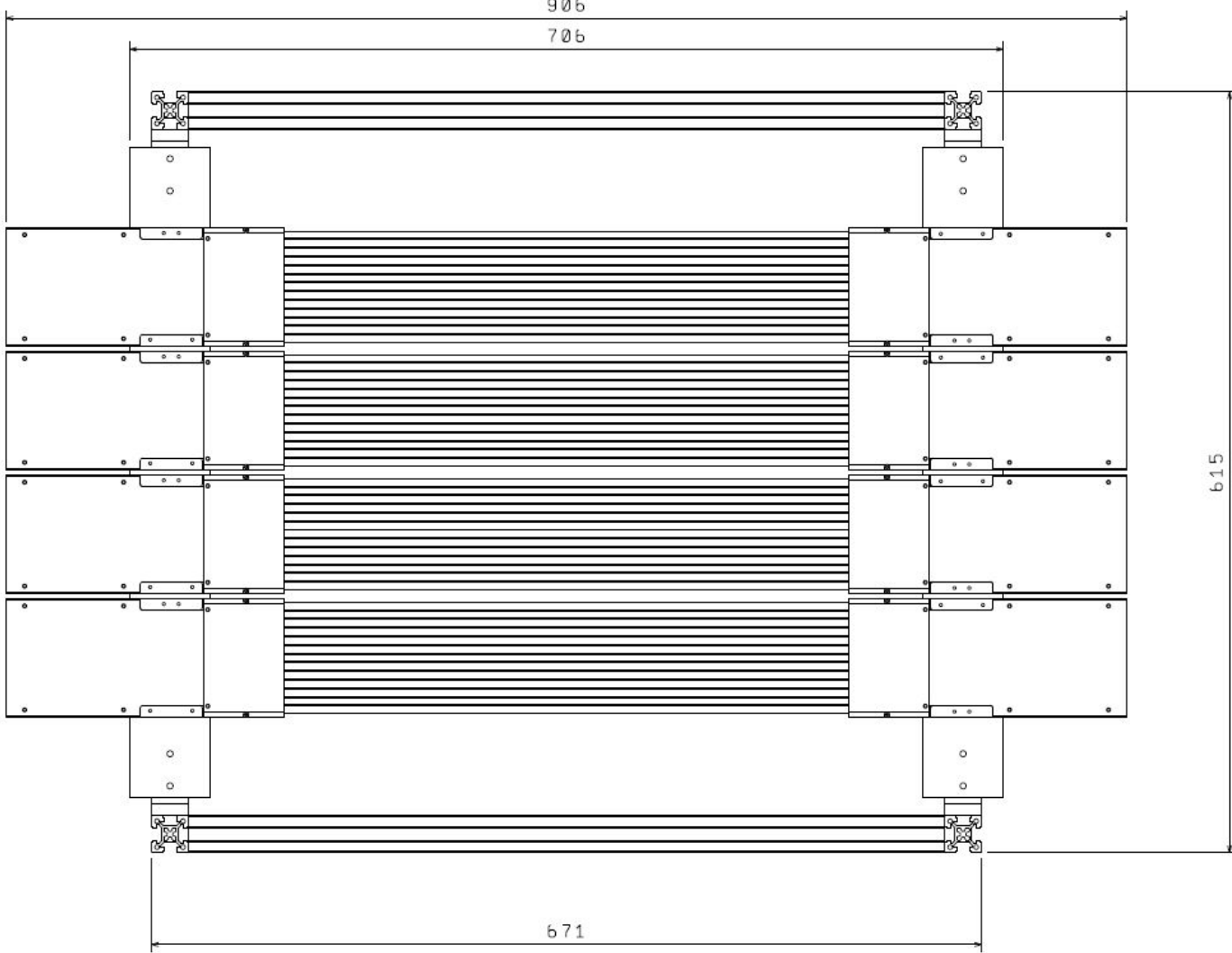
- $20 \times 20 \times 15 \text{ cm}^3$
- 6 mm PMMA walls
- filled with agar + water

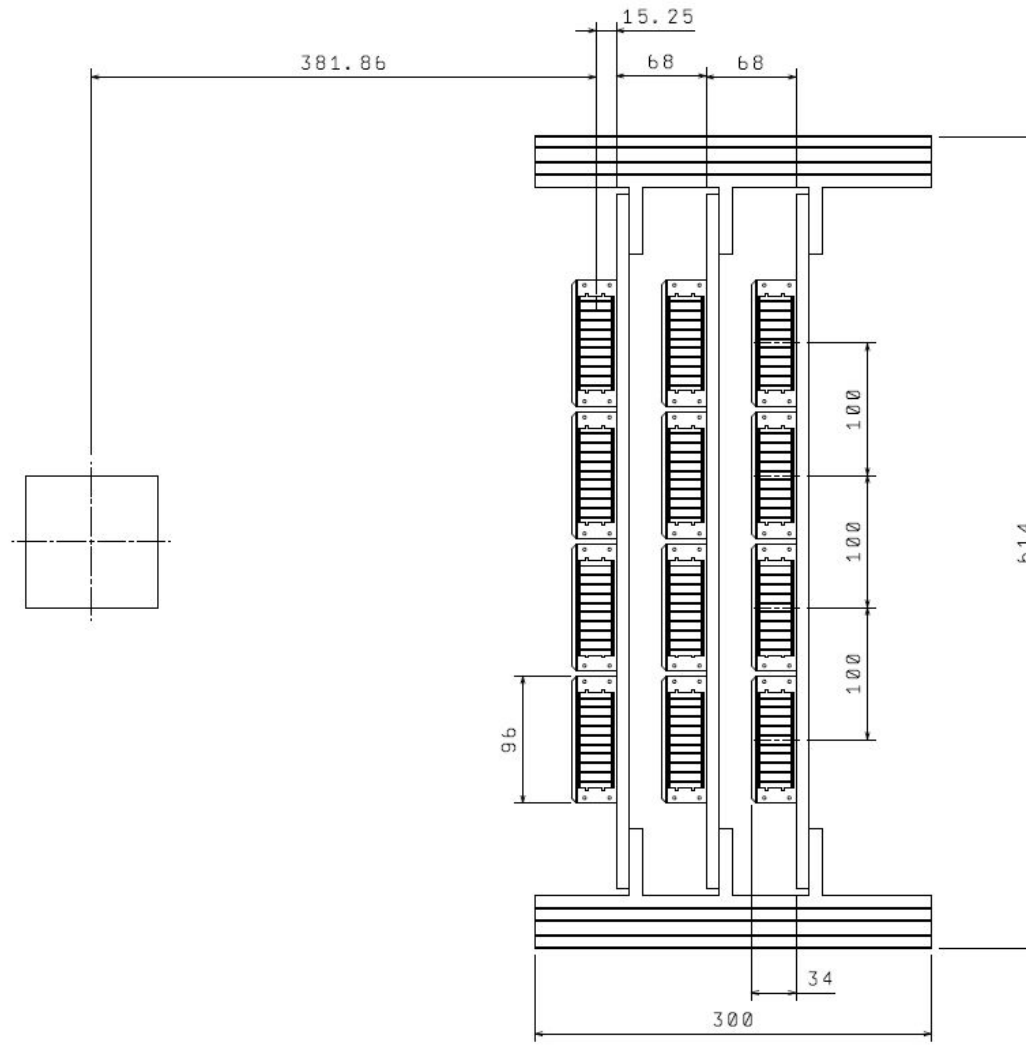


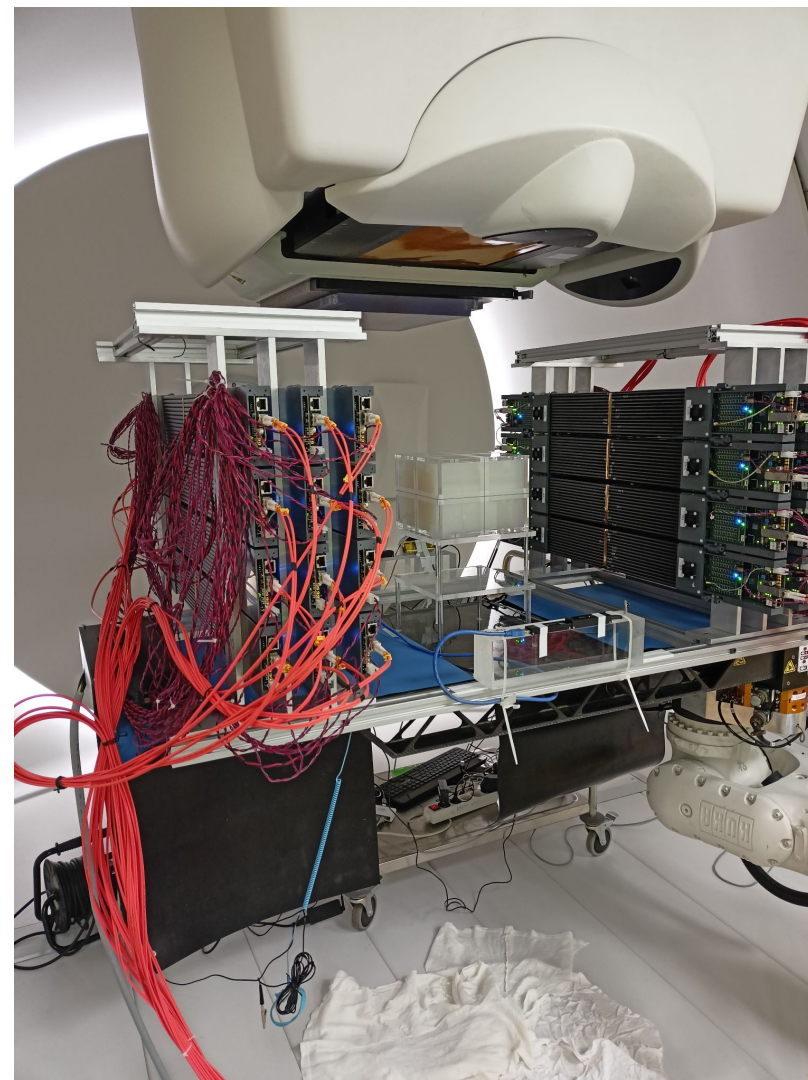
S1F5 and S2F5
40x40 mm² analysed area

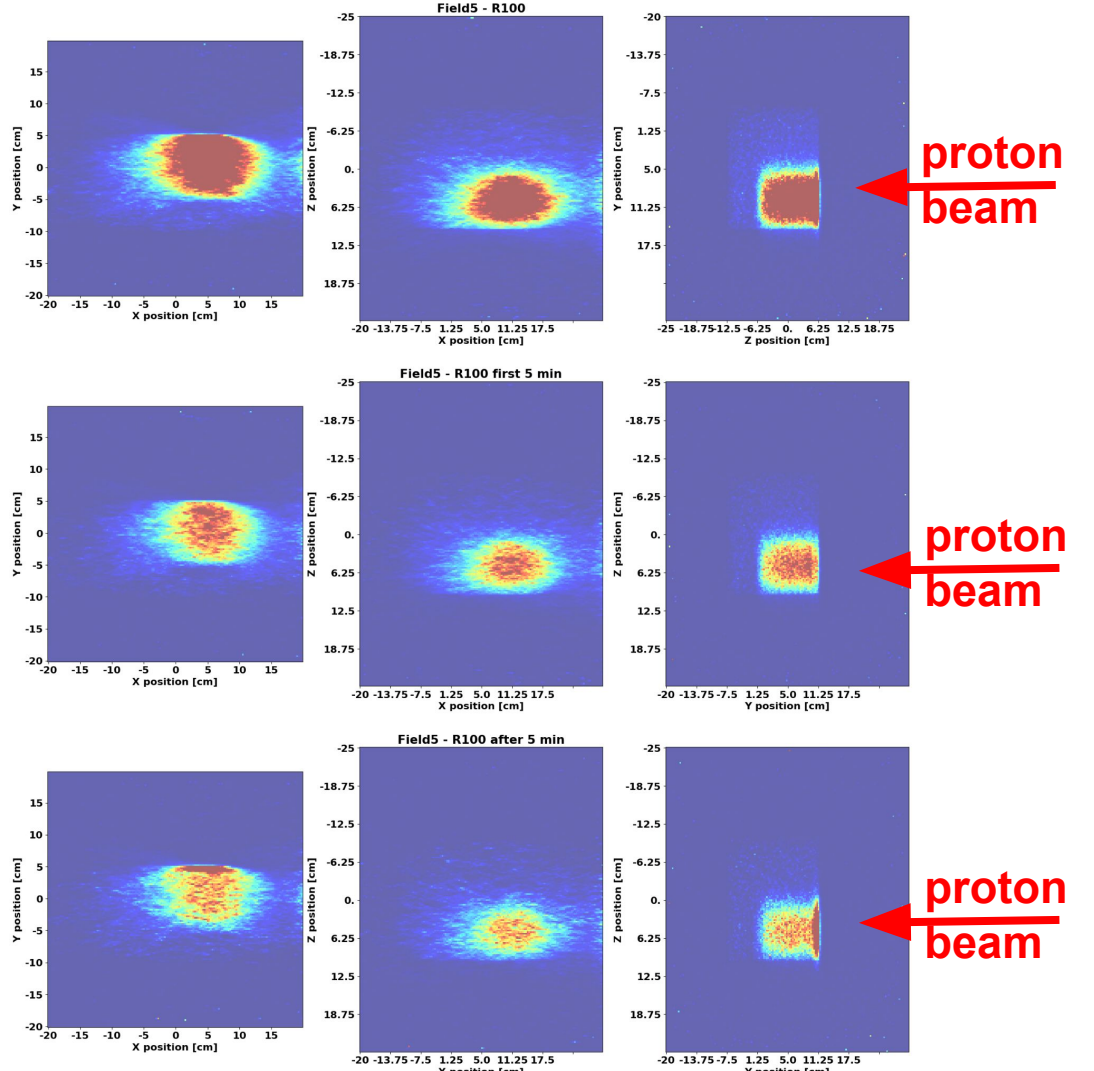


setNo	fieldName	fieldNo	nomRange	range90	range50
1	Field1	1	100	100.40	101.89
1	Field2	2	103	103.61	105.11
1	Field3	3	108	108.47	109.98
1	Field4	4	115	115.17	116.87
2	Field1	1	100	100.38	101.89
2	Field2	2	104	104.60	106.17
2	Field3	3	110	110.51	112.10
2	Field4	4	119	119.41	121.19



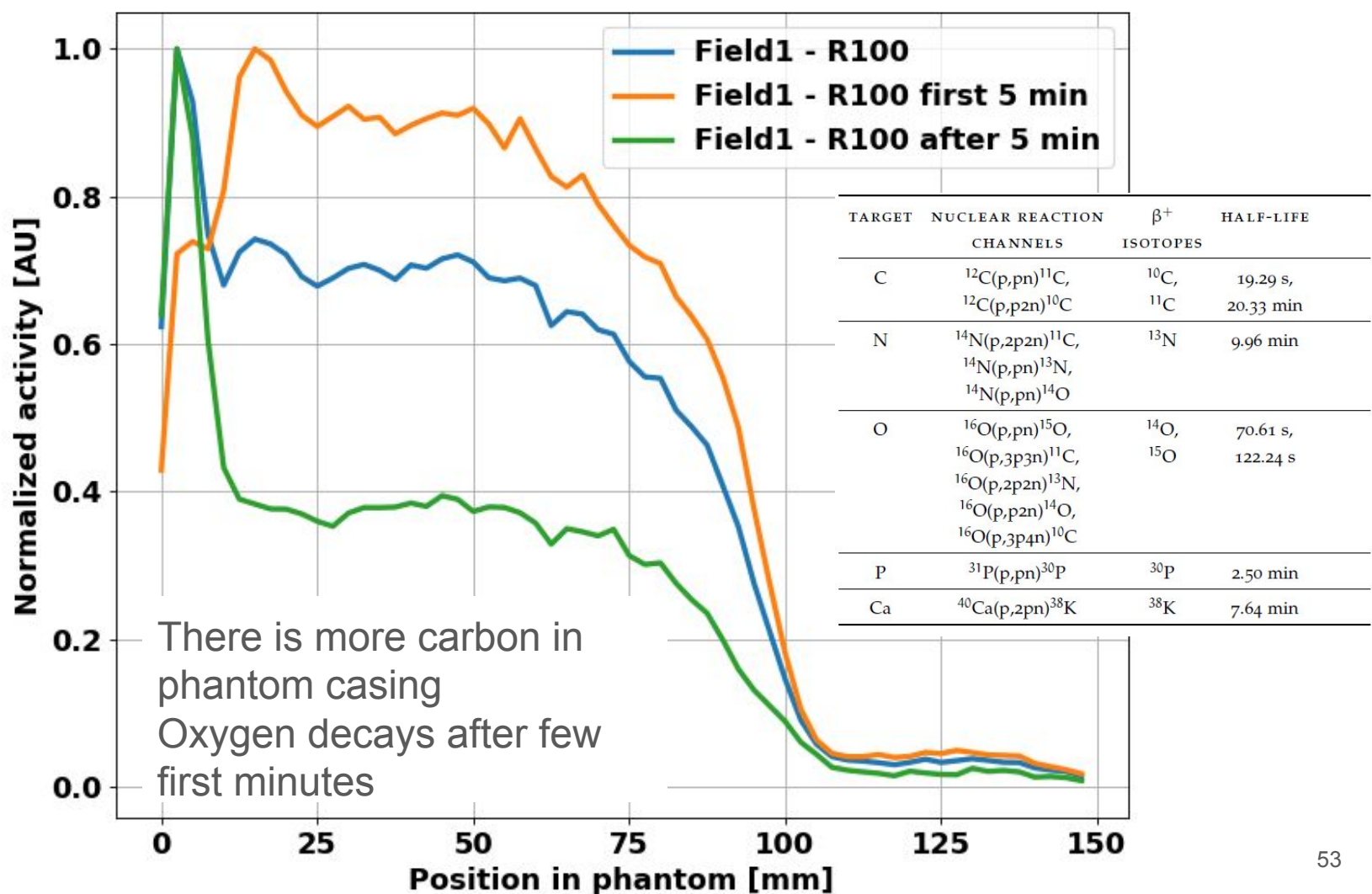






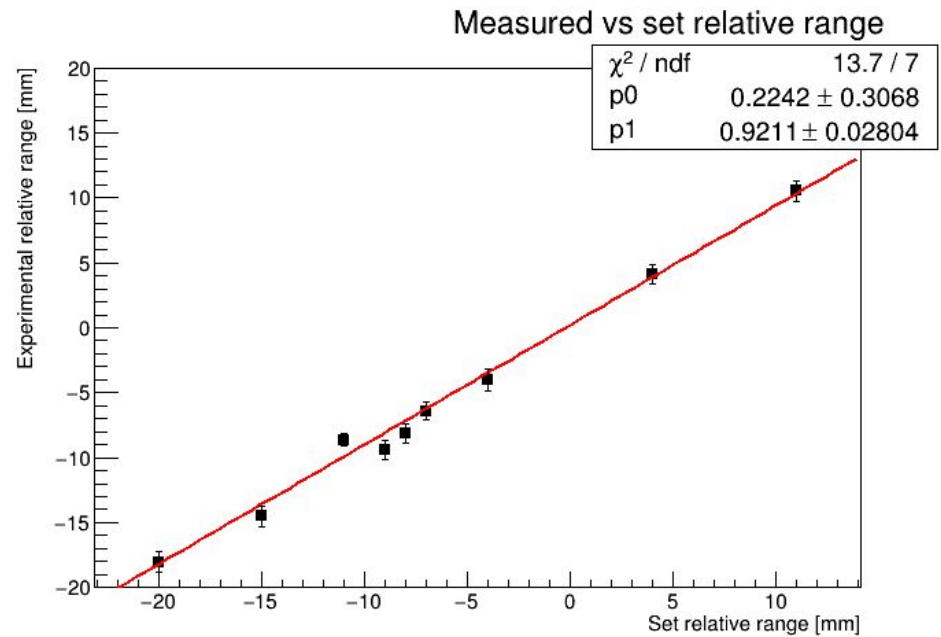
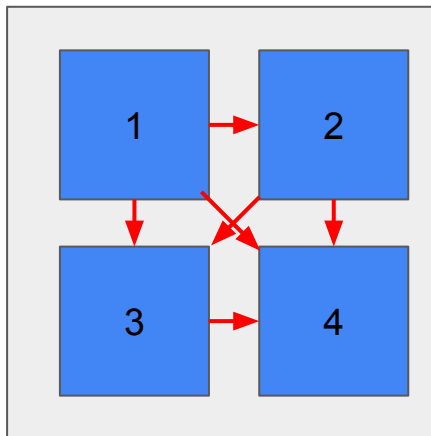
TARGET	NUCLEAR REACTION CHANNELS	β^+	HALF-LIFE
		ISOTOPES	
C	$^{12}\text{C}(\text{p},\text{pn})^{11}\text{C}$, $^{12}\text{C}(\text{p},\text{p}2\text{n})^{10}\text{C}$	^{10}C , ^{11}C	19.29 s, 20.33 min
N	$^{14}\text{N}(\text{p},2\text{p}2\text{n})^{11}\text{C}$, $^{14}\text{N}(\text{p},\text{pn})^{13}\text{N}$, $^{14}\text{N}(\text{p},\text{pn})^{14}\text{O}$	^{13}N	9.96 min
O	$^{16}\text{O}(\text{p},\text{pn})^{15}\text{O}$, $^{16}\text{O}(\text{p},3\text{p}3\text{n})^{11}\text{C}$, $^{16}\text{O}(\text{p},2\text{p}2\text{n})^{13}\text{N}$, $^{16}\text{O}(\text{p},\text{p}2\text{n})^{14}\text{O}$, $^{16}\text{O}(\text{p},3\text{p}4\text{n})^{10}\text{C}$	^{14}O , ^{15}O	70.61 s, 122.24 s
P	$^{31}\text{P}(\text{p},\text{pn})^{30}\text{P}$	^{30}P	2.50 min
Ca	$^{40}\text{Ca}(\text{p},2\text{p}n)^{38}\text{K}$	^{38}K	7.64 min

proton
beam



Remark 2 - make combinations between different fields

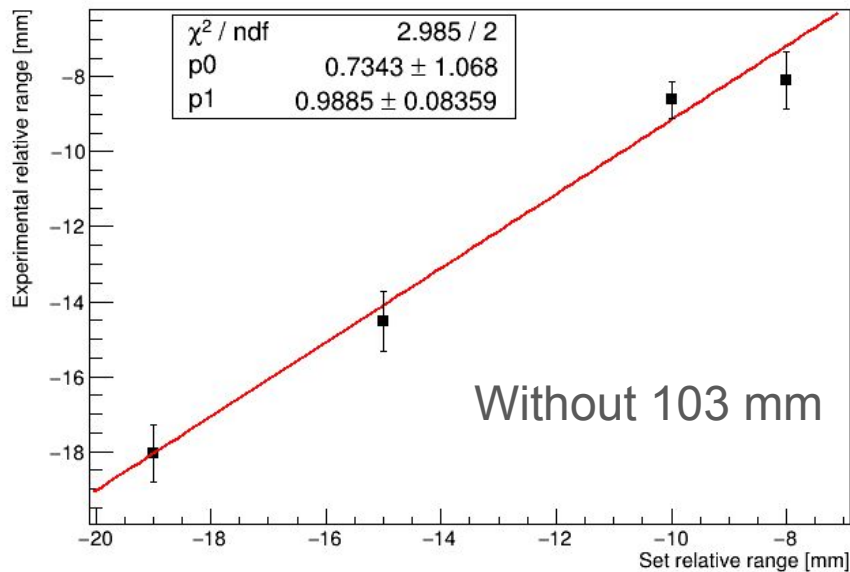
New set of combinations:
1-2; 1-3; 1-4; 2-3; 2-4; 3-4;



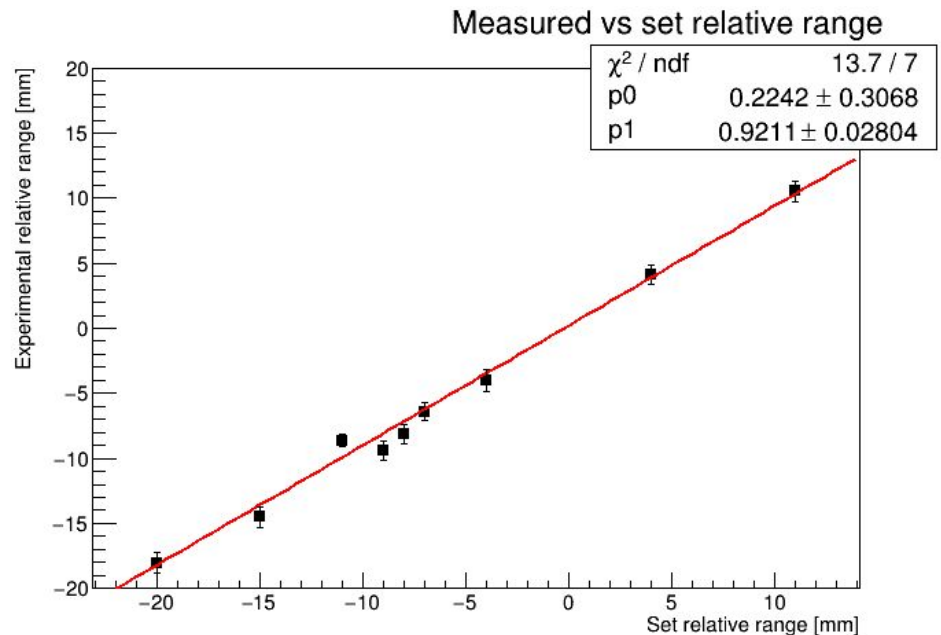
Remark 2 - make combinations between different fields

4 Gy data

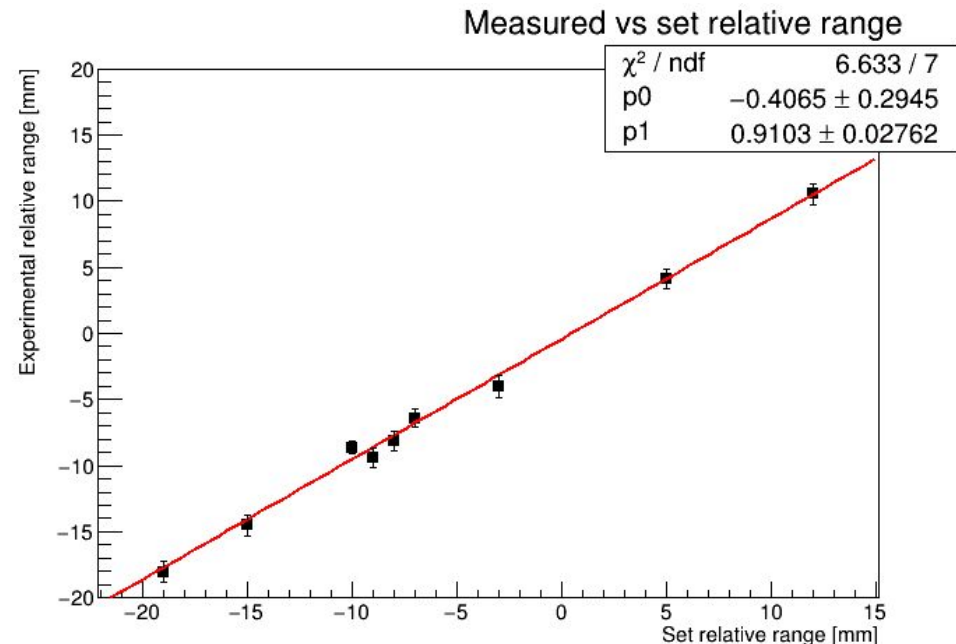
Measured vs set relative range



Measured vs set relative range



Remark 2 - make combinations between different fields ranges from JG



Phantom	Field	Nominal Range [mm]	Range at 50% [mm]	Acquisition time [min]
A	1	100	101.89	30
	2	108	109.98	31
	3	115	116.88	29
	4	103	105.10	30
B	5	100	101.88	33
	6	110	112.10	32
	7	119	121.19	32
	8	104	106.17	35

J-PET experiment at CCB - offline data

S. Niedźwiecki^{b,c}, Antoni Rucinski^a, A. Gajos^{b,c}, G. Korcyl^{b,c}, K. Baran^{b,c}, J. Gajewski^a, P. Stasica^a, K. Brzezinski^{a,d}, D. Borys^{e,f,a}, R. Kopeć^a, Paweł Moskal^{b,c}, author list is there to catch an eye and not in any particular order :) maybe besides the first and the last author

^a Institute of Nuclear Physics PAN, Krakow, Poland

^b Faculty of Physics, Astronomy and Applied Computer Science, Jagiellonian University, S. Łojasiewicza 11, 30-348 Kraków, Poland

^c Total-Body Jagiellonian-PET Laboratory, Jagiellonian University, Poland

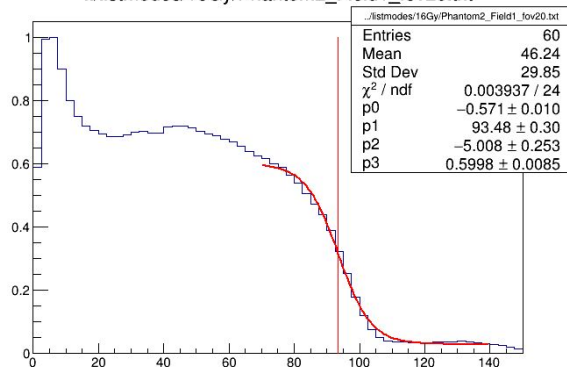
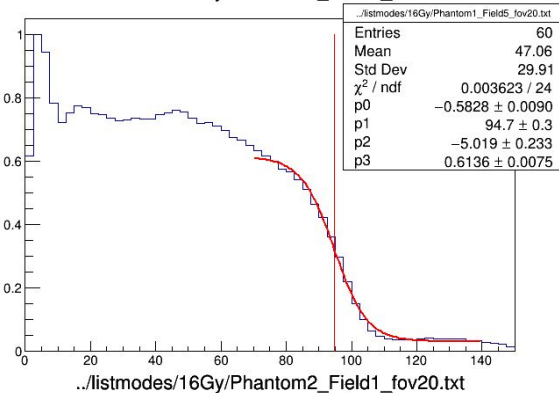
^dInstituto de Física Corpuscular (IFIC), CSIC-UV, Valencia, Spain

^eSilesian University of Technology, Department of Systems Biology and Engineering, Gliwice, Poland

^fBiotechnology Centre, Silesian University of Technology, Gliwice, Poland

Difference between 100 mm range in two phantoms

..//listmodes/16Gy/Phantom1_Field5_fov20.txt



16 Gy data!

R0mm vs FOV

